Laboratory of
WIND ENERGY & TURBULENCE
THE UNIVERSITY OF UTAH

Title: *Comparison of dealiasing schemes in large-eddy simulation of neutrally-stratified atmospheric boundary-layer type flows*

Authors: *Fabien Margairaz, Marco G. Giometto, Marc B. Parlange, and Marc Calaf*

Submitted to: Geosci. Model Dev. (gmd-2017-272)

Reviewer: Anonymous Referee #1

Date: May 1, 2018

General response

Reviewer general comment: *This manuscript addresses the computational cost and the consequences of using different dealiasing schemes in the advective term of the momentum equations for pseudo-spectral discretizations, such as those frequently used in simulations of turbulence in the planetary boundary layer. In particular, two more economical approaches are contrasted with the exact 3/2 rule. Overall the results presented may be relevant for the community interested in turbulence simulation in geophysical settings, such as the planetary boundary layer and the ocean mixed layer. The paper is well written, even though a more concise version would probably be more appealing to the reader. I am a bit surprised by the low cost of the Poisson solver, and the choice of a very low-cost subgrid-scale model certainly helps increasing the share of the convective term on the total cost (as briefly mentioned in the text). After reading the manuscript, I would probably still stick to the 3/2 rule, but that is just my opinion. Having a lower-cost alternative may be useful to other scientists working in the field. The topic may be a bit on the margins of interest of GMD, but I do recommend it for publication. Some important remarks follow below.*

Authors response: We thank the reviewer for his/her positive comments and the recommendation for publication. In this regard the reviewers' comments have made us realize that there were some aspects in the manuscript that required additional clarification and/or improvement. For this reason, down below we provide a clear response to each one of the issues and comments indicated by the reviewer, and an additional explanation on how these have now been addressed within the manuscript.

Based on the comments from both reviewers, we have added a new discussion section to improve the readability of the manuscript. We have also improved the results section by running additional simulations at the resolutions of $192, 192, 128$ and 192^3, as well as running the 256^3-case long enough to be able to report converged statistics. As a result Figures 7, 8 and 9 have been updated, and a new figure (Figure 10) has been included, which is discussed at the end of the results section.

Changes in manuscript: The new discussion section is reported here:

"In the development of this manuscript, focus has been directed to the study of the advantages and disadvantages of different dealiasing methods. In this regard, throughout the analysis we have tried to keep the structure of the LES configuration as simple and canonical as possible, to remove the effect of other add-on complexities. Additional complications might arise when considering additional physics; here we discuss the potential effect that these different dealiasing methods could have on them. One of such elements of added complexity is for example the use of more sophisticated subgrid scale models based on dynamic approaches to determine the values of the Smagorinsky constant (Germano et al., 1991; Bou-Zeid et al., 2005). In most of these advanced subgrid models, information from the small-scale turbulent eddies is used to determine the evolution of the subgrid constant. However, in both the FT and FS method, the small turbulent scales are severely affected and hence use of dynamic subgrid models could be severely hampered unless these are accordingly modified and adjusted, maybe via filtering at larger scales than the usual grid scale. Another element of added complexity consists in using more realistic atmospheric forcing, considering for example the effect of the Coriolis force with flow rotation as a function of height and velocity magnitude. In this case, we hypothesize that the FT method could lead to stronger influences on the resultant flow field as this dealiasing technique not-only affects the distribution of energy in the small turbulent scales, but also in the large scales (as apparent from Fig. 3), being these later ones potentially more affected by the Coriolis force. This represents a strong non-linear effect, that is hard to quantify and hence further testing, including realistic forcing with a geostrophic wind and Coriolis force would be required to better quantify these effects. Also often in LES studies of atmospheric flows one is interested in including an accurate representation of scalar transport (passive/active). In this case the differential equations don't include a pressure term and hence most of the computational cost is linked to the evaluation of the convective term. As a result, the benefit of using alternative, cheaper dealiasing techniques (FT or FS) will be even more advantageous, yet the total gain is not trivial to evaluate *a priori*, and the effect on the scalar fields should also be further evaluated.

In general, we believe that it is not fair to advocate for one or other dealiasing method based on the results of this analysis. Note that the goal of this work is to provide an objective analysis of the advantages and limitations that the different methods provide, letting the readers the ultimate responsibility to choose the option that will adjust better to their application. For example, while having exact dealiasing (3/2-rule) might be better in studies focusing on turbulence and dispersion, one might be well-off using a simpler and faster dealiasing scheme to run the traditionally expensive warm-up runs, or to evaluate surface drag in flow over urban and vegetation canopies, where most of the surface force is due to pressure differences (Patton et al.,2016)."

Specific responses

Major comments:

1. **Reviewer comment:** *The authors perspective on the FT method is a bit different from mine, and to be honest, I am not sure which one is the most prevalent in the community. I have always considered the FT method (which is also known as the $2/3$ rule) as a slightly different implementation of the exact $3/2$ rule, but with a reduced number of effective grid points (actually $N_{eff} = 2N/3$ instead of N). In my view, performing a calculation with $3N/2$ points using the FT method should be identical (in simulation results but maybe not in computational cost) to a simulation with N points using the 3/2-rule, no? I also think the that simulations using the FT method should actually report grid resolution based on N_{eff} and not on N (i.e. the grid spacing should be $\Delta x_{eff} = 3\Delta x/2$ instead of Δx), but that is usually not done. Maybe the authors can comment on this?*

Authors response: This is a very important point in which we fully agree with the reviewer. Running a simulation with $3N/2$ points using the FT method will not provide the same fluid-flow results (physics) than a simulation with N points using the 3/2-rule. The FT method is equivalent of using a coarser grid for the convective term. Therefore, some spurious oscillations appear in the flow field as can be seen in figure 6 of the paper, and indicated therein. In addition, as mentioned also by the reviewer, there will be an important difference in computational cost. For the sake of discussion, we have run a comparison test case with a grid of 128^3 using the 3/2-rule, and another case with a grid of $192, 192, 128$ (so $3N/2$ points in the horizontal direction). Results show that the latter is about 1.65 times more expensive than the former and the physical results are not the same or equivalent either. Specifically, figure 1 shows the instantaneous stream-wise velocity perturbation where some spurious oscillations appear in the flow field. In addition, figure 2 presents the velocity profile, velocity gradient, and variance profiles. The velocity profile obtained with the FT method shows an acceleration of the flow compare to the 3/2-rule, yielding a increase of MKE of 5%. The velocity gradient exhibits a large departure for the FT method at height between $0.2 < z/zi < 0.8$. Similarly, the FT methods yields larger variances throughout the domain.

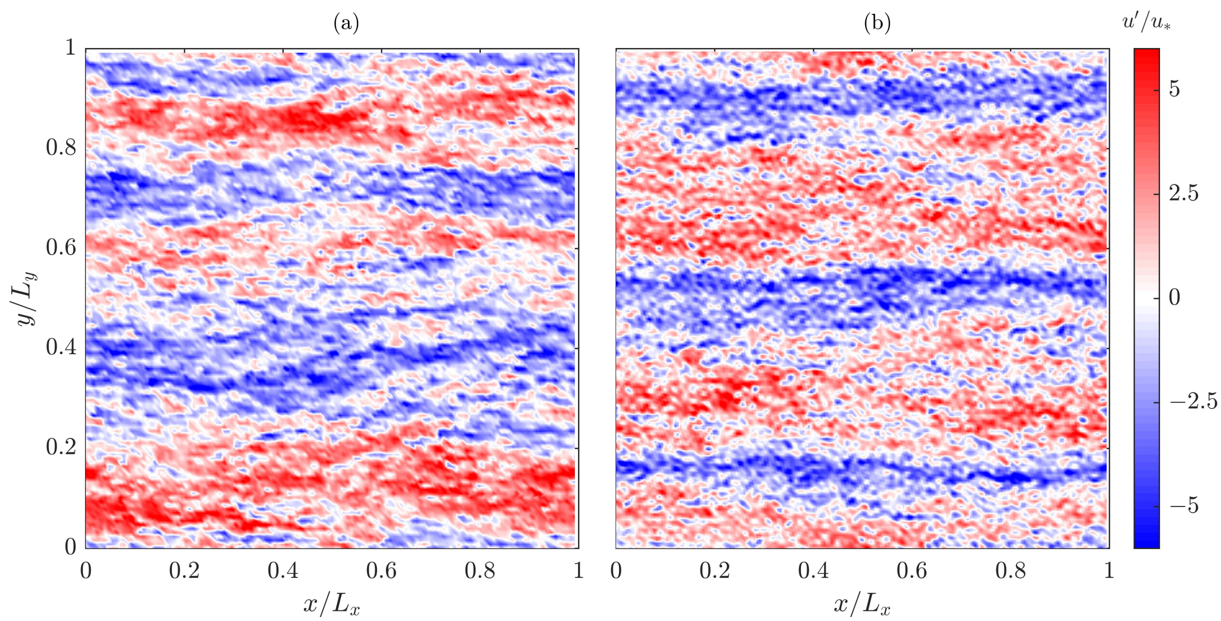

Figure 1: Instantaneous stream-wise velocity perturbation $u'(x, y, z, t) = u(x, y, z, t) - \bar{u}(x, y, z)$ at $z/z_i = 0.054$ for the 128^3-simulation with 3/2-rule (a), and the $192, 192, 128$-simulation with FT (b).

2. **Reviewer comment:** *I am surprised by the high share of the cost carried by the convective term compared to a very low share carried by the Poisson solver. Is this something that is specific to the pencil decomposition parallelization? It may be the case that padding with the 3/2 rule is not as simple in a pencil decomposition approach given that one usually needs to pad the entire 2D "horizontal" wave-number space? Maybe some details of the padding in the context of pencil decomposition would be useful. In addition, is it possible that the Poisson solver is faster when pencil decomposition is used?*

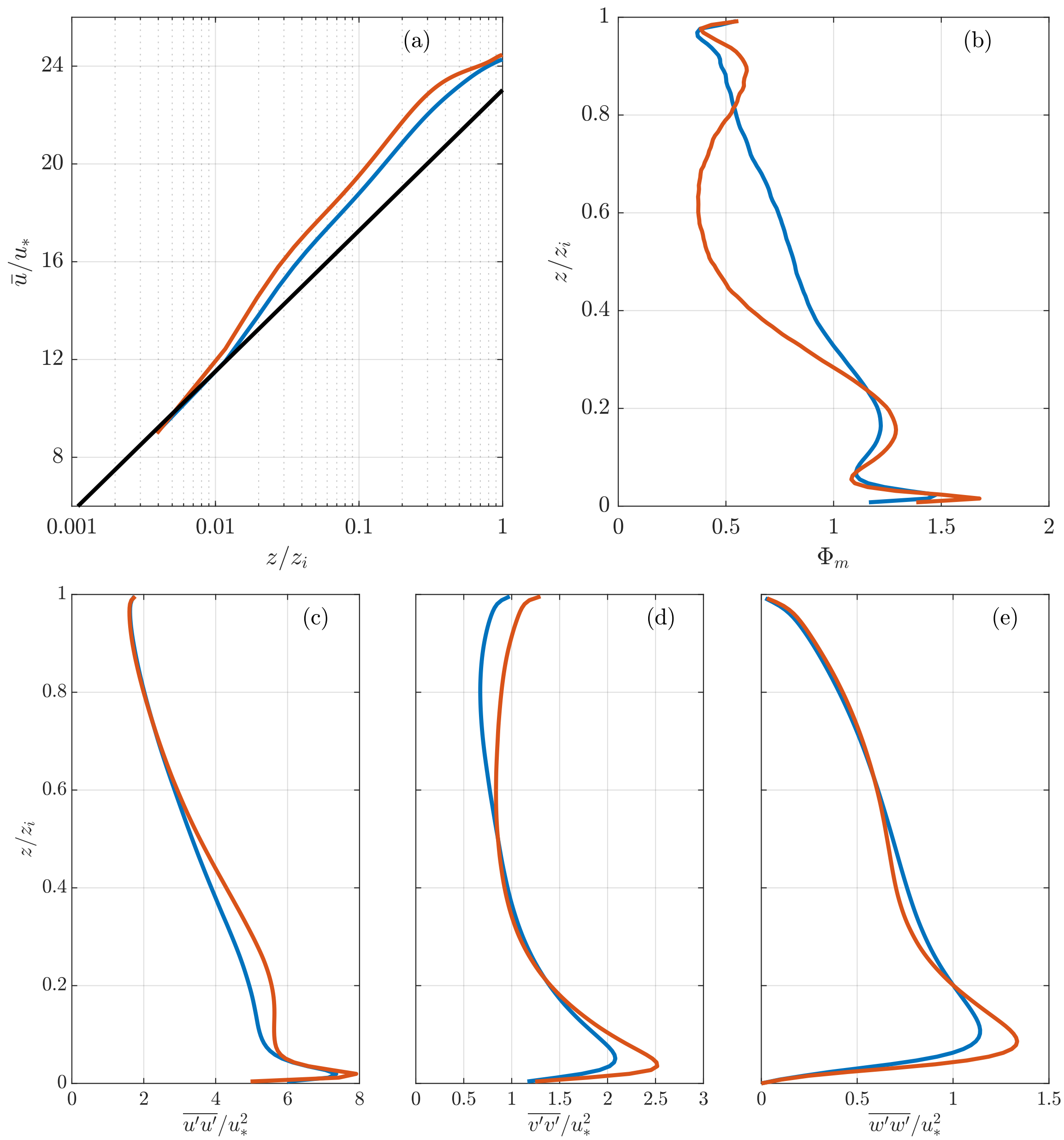

Figure 2: Plots of the non-dimensional mean stream-wise velocity profile (a), the mean stream-wise velocity gradient (b), and the non-dimensional variances (c/d/e). The lines represent the 128^3-simulation with 3/2-rule in blue line and, the $192, 192, 128$-simulation with FT in orange line.

Authors response: Indeed. The cost breakdown for the resolution of the convective term and the Poisson solver is also influenced by the pencil decomposition. In treating the convective term with the pencil decomposition the communication cost increases with respect to the traditional slice parallelization. In this case a total of nine transpositions are needed to compute the convective term, significantly increasing the computational cost.

On the other hand, the Poisson solver becomes faster when using the pencil decomposition in comparison to the slice parallelization. Note that in the pseudo-spectral method the horizontal directions (x and y) are treated in Fourier space and only the vertical direction (z) remains in physical space, therefore each mode in k_x and k_y become independent of each other. In this case the system of equations, originally of size $n_x \times n_y \times n_z$ becomes $n_x \times n_y$ systems of n_z equations, making each vertical line in the domain independent. The pencil decomposition can take full advantage of this fact, making the resolution of the Poisson equation faster. Specifically, once the domain is transposed in the Z-pencil (square pipe aligned with the z-coordinate), the process of solving each of the $n_x \times n_y$ systems does not require any communication, making it very efficient, and limiting its cost to the transposition between the different pencils.

Changes in manuscript: We realize that this is an important detail that should be also mentioned in the manuscript. For this reason we have included a couple of lines in section 3.3.

The text now reads as:"In addition, it is important to note that the low computational cost of the Poisson solver is related to the the use of the pencil decomposition, which takes full advantage the pseudo-spectral approach. Specifically, the Z-pencil combines with the horizontal treatment of the derivatives to make the implementation of the solver very efficient."

3. **Reviewer comment:** *The quantification of computation cost in section 4.1 is fine. Regarding the results in section 4.2, I wonder if the question could be posed the other way around. In my view, maybe the most relevant question would be: "given a set computational cost, do I get better results (a) using the $3/2$ rule or (b) running a finer grid using a less expensive dealiasing?". I know the experiment is not easy to design (because one needs to estimate the computational cost ahead of time), but that seems to be the more important question to be answered. If I save 30% on dealiasing and spend it on more resolution, do I get better results? From my comment above, I would expect that the FT method is almost equivalent to the $3/2$ rule (if smartly coded). How about the FS?*

   Authors response: This is a very interesting point that is being raised. It is true that *a-priory*, as the reviewer mentions, one could compute the associated computational gain linked to using the FT method and decide using a finer grid that would 'use' the time resources saved in the benefit of resolution. However this is a challenging endeavor for many different reasons. For example, if one was to consider an a-priory 20% gain when using the FT method on a given numerical grid of 128^3 points, and decided to use a more resolved grid to 're-invest' the saved computational resources, then one would have to use a grid of ~ 150 $(128 + 0.2 \times 128)$. Unfortunately, this number of grid points will not work well with the FFT given that it's not a power of 2 and hence will induce a slow down of the computations. Accounting for this factor is quite challenging, if not unfeasible, turning the reviewer's suggestion in a very hard challenge. In this regard, also note the response to the first point raised where it is clarified the fact that the 3/2 rule does not provide the exact same results to the case using the 2/3 rule with an equivalently larger grid.

   Alternatively, the gain in computational time could be for example invested in running longer simulations, or reduce the time in 'warm-up' configurations.

   Changes in manuscript: We have included an additional comment related to the possible use of the FT or FS method as precursor simulations in the new discussion section (reported above).

4. **Reviewer comment:** *Regarding the interpretation of Figure 7. I am not convinced the log-law prediction is as good as described in the text (but perhaps I am missing something here?). First, it seems that there is one log-law on top of the solid line that may extend only for 2 or 3 vertical levels (ending around $z/z_i \leq 0.02$). Then there is a second log-law (only in $3/2$ and FT cases) that starts*

around $z/z_i = 0.04$ and goes beyond $z/z_i = 0.1$, This second log-law has the incorrect roughness (if one were to extrapolate it to $u = 0$, it would yield a lower value of z_0 than the one imposed on the simulation, I think). There is no clear second log-law in the FS method. I would see this as a concern for the FS method (which is being advocated here), except that not even the exact 3/2 rule has a good log-law (as seen in Bou-Zeid et al, 2005). I am pretty sure this is due to the SGS model adopted here. In any case, if I had to choose between the FS and FT methods based on Figure 7, I would probably go with FT, since it does a reasonable job in the lower 20% of the domain (which is the region of interest in a simulation like this, I guess). Also, the FS method seems more over-dissipative near the wall (on panel b), which is opposite to what is described in the text?

Authors response: We agree with the reviewer that the log-law predictions are far from perfect, yet they match well with those presented in Bou-Zeid et al, (2005) when using the constant Smagorinsky coefficient (contrasted on a side work). This means that the deviations from the theoretical log-law are mostly due to the SGS model, as the reviewer suggests. These deviations are more prominent in the FS method whereas the FT shows excellent agreement with predictions from the 3/2-rule in the surface layer.

In regards to the second comment, we believe that there was a misunderstanding, given that the authors comments in the manuscript referred to the upper region of the BL, while the reviewer is referring to the surface layer region.

Changes in manuscript: We have now clarified both issues in the revised version of the manuscript. The interpretation of the figure 7 now reads:
"The horizontally- and temporally-averaged velocity profiles are characterized by an approximately logarithmic behavior within the surface-layer ($z \approx 0.15z_i$, as apparent from Fig. 7, where results are illustrated for the three resolutions: 128^3,192^3, and 256^3). For the 128^3 case, the observed departure from the logarithmic profile for the 3/2-rule case is in excellent agreement with results from previous literature for this particular SGS model (Port-Agel et al., 2000; Bou-Zeid et al., 2005). When using the FT method the agreement of the averaged velocity profile with the corresponding 3/2-rule profiles improves with increasing resolution. While in the 128^3 case a good estimation of the logarithmic flow is obtained at the surface layer, there is a large acceleration of the flow further above. This overshoot does not occur for the higher resolution runs. When using the FS method, the mean velocity magnitude is consistently over-predicted throughout the domain, and the situation does not improve with increasing resolution (the overshoot is up to 7.5% for the 128^3, 8.5% for the 192^3 and 7% for the 256^3 run). Further comparing the results obtained by the FS and FT method with those obtained with the 3/2-rule, it is clear that while the FS method presents a generalized overestimation of the velocity with a an overall good logarithmic trend, the FT method presents a better adjustment in the surface layer with larger departures from the logarithmic regime on the upper domain region that get reduced with increasing numerical resolution. The mean kinetic energy of the system is overestimated by $\approx +2\%$ and $\approx +12\%$ by the FT and FS methods, when compared to that of runs using the 3/2-rule in the 256^3 case. Overall, the mean kinetic energy is larger for the FT and FS cases, when compared to the 3/2-rule case, even at the highest of the considered resolutions ($\approx +2\%$ and $\approx +12\%$ by the FT and FS methods for the 256^3 case). Such behavior can be related to the low-pass filtering operation that is performed in the near-wall regions, which tends to reduce resolved turbulent stresses in the near-wall region, resulting in a higher mass flux for the considered flow system. This is more apparent for the low resolution cases.

Mean velocity gradient profiles ($\Phi_m = \kappa \frac{z}{u_*} \partial_z \langle U \rangle_{xy}(z)$) are also featured in Figure 7 (d, e, f). Profiles at each of the considered resolutions present a large overshoot near the surface, which is a well known problem in LES of wall-bounded flows and has been extensively discussed in the literature (Bou-Zeid et al., 2005; Brasseur and Wei, 2010; Lu and Port-Agel, 2013). In comparing the results between the FS and FT method with the 3/2-rule, it can be observed that there are stronger gradients in the mean velocity profile within the surface layer when using the FS method. This leads to the observed shift in the mean velocity profile. Conversely, when using the FT method, departures are of oscillatory nature, leading to less pronounced variations in the mean velocity profile when compared to the reference ones (the 3/2-rule cases). This behavior is consistently found across the considered resolutions, but the situation ameliorates as resolution is increased (*i.e.* weaker departures)."

5. **Reviewer comment:** *Regarding Figure 9. I do not agree that the filtering only affects the small-scale end of the spectra. For the FT case, it seems clear to me that there is significant damping of the large scales as well. This is related to the underestimation in the variance of the streamwise velocity seen in Figure 8. This is worrisome, and probably related to the fact that the true resolution here ($N_{eff} = 85$ points) is too coarse to model the ABL. I wonder if this situation would persist in the 256^3 simulations?*

   Authors response: Thank you very much, this is a very interesting and important point. The underestimation of the variance of the streamwise velocity did not persist in the 256^3 simulations. In addition, to clarify the effect of the FT and FS methods on the spectra, we have developed an additional analysis using the spectra presented in the paper. Although the effect of the FT and FS methods on the small scales can be clearly observed on the spectra, their effect on the large scales cannot be directly assessed from the figure, as pointed out by the reviewer. To compute a direct comparison scale by scale, the following ratio was used for the 128^3, 192^3, and 256^3-simulations,

$$\rho^{XX}(k) = \frac{E_{u,k}^{XX} - E_{u,k}^{3/2}}{E_{u,k}^{3/2}} \tag{1}$$

   where $E_{u,k}$ denotes the power spectral density of the u velocity component at wavenumber k, XX stands for the dealiasing method FT or FS. Hence, if $\rho(k) < 0$ energy is removed at that scale, and if $\rho(k) > 0$ energy is added at that scale. Figure 3 presents the ratio $\rho(k)$ for both methods where it can be observed that the effect of FT methods is very large at all scales. The large scales ($0 \leq k/k_{max} \leq 0.2$) are affected with a reduction of energy of ∼25%. The mid-range scales ($0.2 \leq k/k_{max} \leq 0.6$), corresponding to the inertial sub-range, exhibit an overestimation of their energy of about ∼50% on average. Therefore, this method redistributes the energy of the small scales into the inertial sub-range scales. On the contrary, in the FS method, the energy from the filtered small-scales is redistributed more or less uniformly throughout with an averaged overall variation of less the 13%.

   Changes in manuscript: We have added figure 3 and its interpretation in the manuscript. This now reads as: "Although the effect of the FT and FS methods on the small scale can be clearly observed in figure 9, their effect on the large scales also needs to be quantified. To compute a direct comparison scale by scale, the following ratio was used (equation 1) for the 128^3, 192^3, and 256^3-simulations,

$$\rho^{XX}(k) = \frac{E_{u,k}^{XX} - E_{u,k}^{3/2}}{E_{u,k}^{3/2}} \tag{2}$$

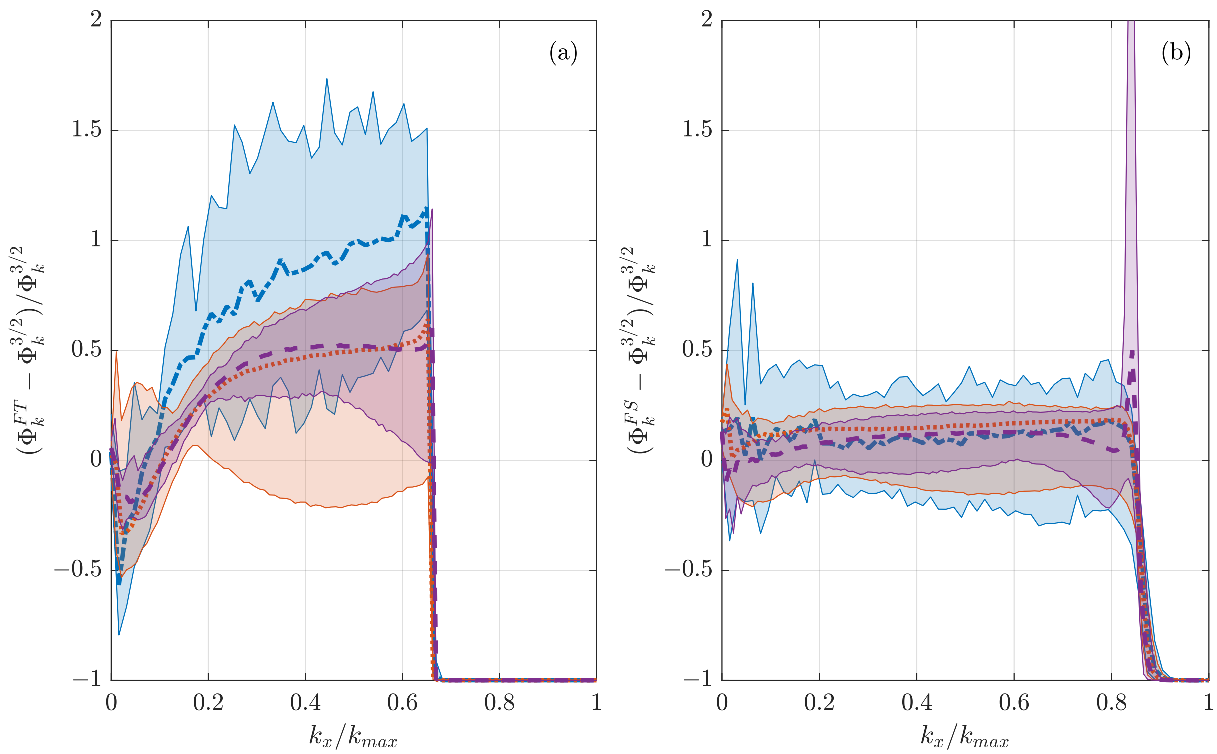

Figure 3: Effect of the FT (a), and the FS (b) methods of the stream-wise spectra of the stream-wise velocity compare to the 3/2-rule. The solid line represent the average value and the shaded area represent the extreme values. The resolutions are: 128^3 in blue dot-dashed line, 192^3 in red dotted line, and 256^3 in purple dashed line.

where $E_{u,k}$ denotes the power spectral density of the u velocity component at wavenumber k, XX stands for the dealiasing method FT or FS. If $\rho(k) < 0$ the energy density at that given wavenumber (k) is less than the corresponding one for the run using the $3/2$ rule, viceversa if $\rho(k) > 0$. Figure 3 presents the ratio $\rho(k)$ for both methods.

When using the FT method, energy at the low wavenumbers is underpredicted, whereas energy at the large wavenumbers is overpredicted. Departures are in general larger with decreasing resolution, with an excess of up to 100% for the 128^3-simulations in the wavenumber range close to the cutoff wavenumber. On the contrary, when using the FS method, the energy from the filtered (dealiased) small-scales is redistributed quasi-uniformly throughout the spectra with an averaged overall variation of less than 13%.”

6. **Reviewer comment:** *I see two facts that could benefit from more discussion in the manuscript (maybe in the conclusions):*
(a) The importance of reducing computational cost in the advection term for simulations that use more sophisticated SGS models (maybe this can be brought up again in the conclusions?)
(b) The consequence for including one or many additional scalar fields (temperature, water vapor, etc.). These also require dealising and do not require additional pressure solvers and/or very expensive SGS models. I would probably anticipate that in simulations with several scalars, the savings would be significantly larger. Is that correct?

Authors response: Thank you, (a) is a great point. In this regard, we have now run some additional simulations using the dynamic Smagorinsky model. Results are illustrated in Figure 4. In this figure, it can be observed that the dynamic model fails to compute the Smagorinsky constant when using either the FS or the FT methods. In addition, the FT methods strongly suppresses the turbulence, resulting in the lamieraizition of the flow. Alternatively, the consequences of using the FS method are less dramatic, although the flow also exhibits a large acceleration at the top of the domain. As mentioned by the reviewer, these results are not surprising given that the dynamic models are using a relation between the small scales to compute the Smagorinsky constant. Therefore, the FT and FS methods cannot be used

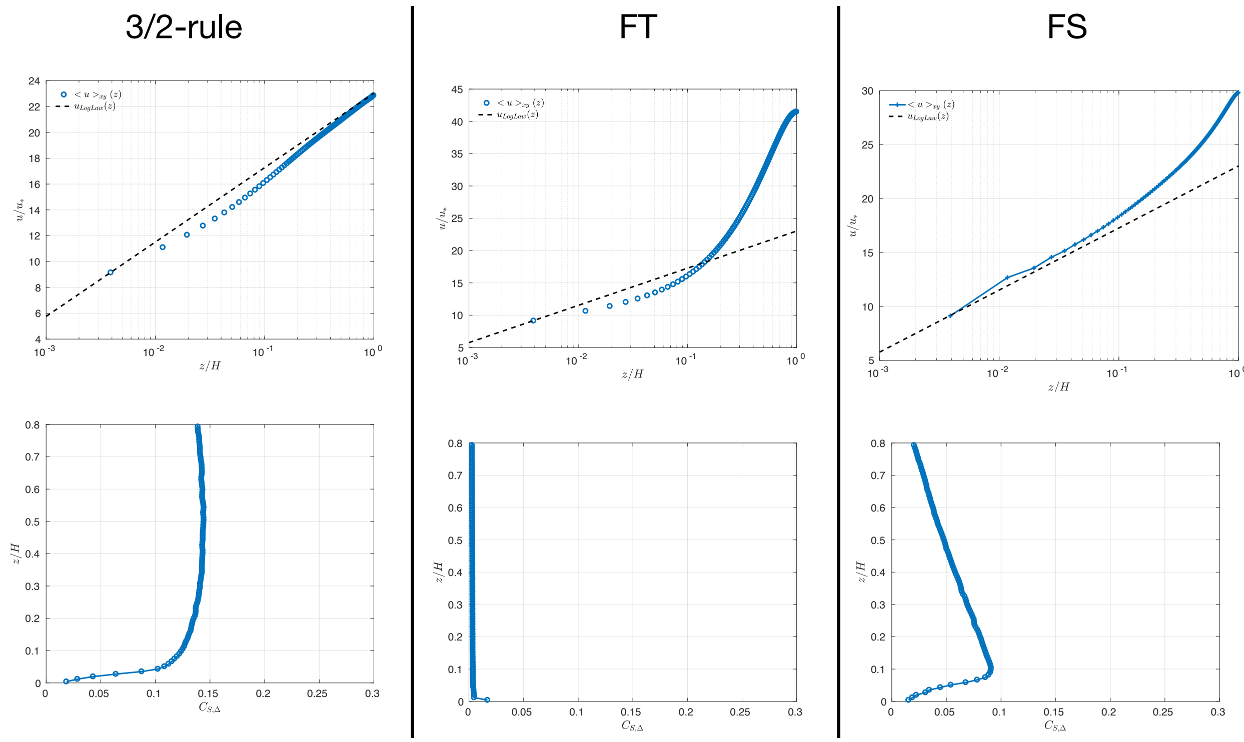

Figure 4: Profiles of the horizontal velocity and the Smagorinsky constant for the three deasliasing methods at a resolution of 128^3.

with dynamic SGS models unless the dynamic models are properly adjusted with filtering at scales larger than those affected by the truncation or smoothing. Therefore, it is impossible to *re-invest* the computation gain due to the FT or FS methods into a more sophisticate SGS model (at lease not a dynamic Smagorinsky-type model from Germano (1991)).

In relation to the second comment, adding extra scalars will decrease the cost of the momentum solver with respect to the total cost of the simulation. Each scalar field is advanced in time using an advection-diffusion equation that also requires dealiasing. However, the cost of the dealiasing of the latter equation is less expensive than the NS equations (especially in rotational form). To summarize, each dealiasing operation becomes less expensive with the FT or FS method, and the total gain will be more important as more operations are required. However, the total gain is not trivial to evaluate *a priori*.

Changes in manuscript: We agree that both issues are relevant, and hence we have included some additional comment in the new discussion section (reported above).

Minor comments:

1. **Reviewer comment:** *Page 4, Line 33 - please check that the N^3 term in the cost is correct here.*

   Authors response: Thank you for pointing out this mistake. This cost should not have a N^3 but only N.

2. **Reviewer comment:** *Page 5, Line 10 - delta implicit does not really correspond to a top-hat filter. The properties of an implicit filter are tied to the discretization scheme. As an example, for a true 3D spectral code the implicit filter is a spectral cutoff filter.*

   Authors response: Thank you this is a good point. This has been corrected in the text.

Title: *Comparison of dealiasing schemes in large-eddy simulation of neutrally-stratified atmospheric boundary-layer type flows*

Authors: *Fabien Margairaz, Marco G. Giometto, Marc B. Parlange, and Marc Calaf*

Submitted to: Geosci. Model Dev. (gmd-2017-272)

Reviewer: Referee #2

Date: May 1, 2018

General response

Reviewer general comment: *The paper compares various approaches for the dealiasing of the non-linear terms in large eddy simulation of atmospheric flows. Given that spectral methods are widely used in studying such flows under idealized conditions since they offer higher speed and better accuracy, the general theme is of interest to GMD readers. The paper does a good job in presenting the fundamentals of the problem, the proposed solutions, and how they compare when implemented in an actual code. But major revisions are needed. In particular, the study is a valuable comparison of the methods that is not available (to the best of my knowledge) in the literature and the authors should not try to conclude that one is more optimal than the others. They can simply present their findings and let the users determine which method is suitable for their needs.*

Authors response: We thank the reviewer for his/her valuable comments and for recommending publication of the manuscript. In this regard we have taken good note of the reviewer comments, which have been addressed in detail below.

Based on the comments from both reviewers, we have added a new discussion section to improve the readability of the manuscript. We have also improved the results section by running additional simulations at the resolutions of $192, 192, 128$ and 192^3, as well as running the 256^3-case long enough to be able to report converged statistics. As a result Figures 7, 8 and 9 have been updated, and a new figure (Figure 10) has been included, which is discussed at the end of the results section.

Changes in manuscript: The new discussion section is reported here:

"In the development of this manuscript, focus has been directed to the study of the advantages and disadvantages of different dealiasing methods. In this regard, throughout the analysis we have tried to keep the structure of the LES configuration as simple and canonical as possible, to remove the effect of other add-on complexities. Additional complications might arise when considering additional physics; here we discuss the potential effect that these different dealiasing methods could have on them. One of such elements of added complexity is for example the use of more sophisticated subgrid scale models based on dynamic approaches to determine the values of the Smagorinsky constant (Germano et al., 1991; Bou-Zeid et al., 2005). In most of these advanced subgrid models, information from the small-scale turbulent eddies is used to determine the evolution of the subgrid constant. However, in both the FT and FS method, the small turbulent scales are severely affected and hence use of dynamic subgrid models could be severely hampered unless these are accordingly modified and adjusted, maybe via filtering at larger scales than the usual grid scale. Another element of added complexity consists in using more realistic atmospheric forcing, considering for example the effect of the Coriolis force with flow rotation as a function of height and velocity magnitude. In this case, we hypothesize that the FT method could lead to stronger influences on the resultant flow field as this dealiasing technique not-only affects the distribution of energy in the small turbulent scales, but also in the large scales (as apparent from Fig. 2), being these later ones potentially more affected by the Coriolis force. This represents a strong non-linear effect, that is hard to quantify and hence further testing, including realistic forcing with a geostrophic wind and Coriolis force would be required to better quantify these effects. Also often in LES studies of atmospheric flows one is interested in including an accurate representation of scalar transport (passive/active). In this case the differential equations don't include a pressure term and hence most of the computational cost is linked to the evaluation of the convective term. As a result, the benefit of using alternative, cheaper dealiasing techniques (FT or FS) will be even more advantageous, yet the total gain is not trivial to evaluate *a priori*, and the effect on the scalar fields should also be further evaluated.

In general, we believe that it is not fair to advocate for one or other dealiasing method based on the results of this analysis. Note that the goal of this work is to provide an objective analysis of the advantages and limitations that the different methods provide, letting the readers the ultimate responsibility to choose the option that will adjust better to their application. For example, while having exact dealiasing (3/2-rule) might be better in studies focusing on turbulence and dispersion, one might be well-off using a simpler and faster dealiasing scheme to run the traditionally expensive warm-up runs, or to evaluate surface drag in flow over urban and vegetation canopies, where most of the surface force is due to pressure differences (Patton et al.,2016)."

Specific responses

Major comments:

1. **Reviewer comment:** *While the FS method seem to be giving an acceptable performance as the authors argue, I wonder whether the ABL LES community should be going in a direction of saving computing time rather than maximizing the accuracy of the computation. We push for higher resolution to gain better accuracy and, with increasing computing power, I wonder whether a 20% drop in simulation time is worth it. We use dynamic SGS models that increase the computing time by 20% all the time. The plots in Fig 7 do not indicate that the FS method is as good as the 3/2 method. So in general I think the authors should not focus on the conclusion that the FS method is a good surrogate. They should present the information and findings, which will help modelers decide on the trade offs they want (on my end this convinces me that using a 3/2 method is indeed worth it.).*

   Authors response: Thanks, we indeed agree with the reviewer's point. We believe that gaining a 20% in computational time can be of interest in certain occasions, for example during warm up periods. However, as the reviewer mentions the strength of this manuscript should reside on conveying the facts of using different dealiasing methods, and allowing the corresponding end users to decide what's best for them according to their application.

Changes in manuscript: To clarify this point we have added a discussion section (reported above) and rewritten the conclusion section. The new conclusion section emphasize the trade offs of each method. The modifications to conclusion reported here:

"The Fourier-based pseudo-spectral collocation method (Orszag, 1970; Orszag and Pao, 1975; Canuto et al., 2006) remains the preferred "work-horse" in simulations of wall-bounded flows over horizontally periodic regular domains, which is often used in conjunction with a centered finite-difference or Chebychev polynomial expansions in the vertical direction (Shah and Bou-Zeid,2014; Moeng and Sullivan, 2015). This approach is often used because of the high-order accuracy and the intrinsic efficiency of the fast-Fourier-transform algorithm (Cooley and Tukey, 1965; Frigo and Johnson, 2005). In this technique, aliasing that arises when evaluating the quadratic non-linear term in the NS equations can severely deteriorate the quality of the solution and hence need to be treated adequately. In this work a performance/cost analysis has been developed for three well-accepted dealiasing techniques (3/2-rule, FT and FS) to evaluate the corresponding advantages and limitations. The 3/2-rule requires a computationally expensive padding and truncation operation, while the FT and FS methods provide an approximate dealiasing by low-pass filtering the signal over the available wavenumbers, which comes at a reduced cost.

The presented results show compelling evidence of the benefits of these methods as well as some of their drawbacks. The advantage of using the FT or the FS approximate dealiasing methods is their reduced computational cost ($\sim$15% for the 128^3 case, $\sim$25% for the 256^3 case), with an increased gain as the numerical resolution is increased. Regarding the flow statistics, results illustrate that both, the FT and the FS methods, yield less accurate results when compared to those obtained with the traditional 3/2-rule, as one could expect.

Specifically, results illustrate that both the FT and FS methods over-dissipate the turbulent motions in the near wall region, yielding an overall higher mass flux when compared to the reference one (3/2-rule). Regarding the variances, results illustrate modest errors in the surface-layer, with local departures in general below 10% of the reference value across the considered resolutions. The observed departures in terms of mass flux and velocity variances tend to reduce with increasing resolution. Analysis of the streamwise velocity spectra has also shown that the FT method redistributes unevenly the energy across the available wavenumbers, leading to an over-estimation of the energy of some scales by up to 100%. Contrary, the FS methods redistributes the energy evenly, yielding a modest +13% energy magnitude throughout the available wavenumbers. Compared to the 3/2-rule, these differences in flow statistics are the result of the sharp low-pass filter applied in the FT method and the smooth filter that characterizes the FS method."

2. **Reviewer comment:** *How do the FT and FS method influence the potential use of dynamic models that require good accuracy on the smallest resolved scales? If as the spectra show they damp these scales, than that would preclude using dynamic models and would be a significant disadvantage of FT and FS. The authors have in their code some dynamic models, they could perform the dynamic computations while still using the Static Smagorinsky (compute a dynamic Cs but dont use it).*

   Authors response: Thank you, this is a great point. In this regard, we have now run some additional simulations using the dynamic Smagorinsky model. Results are illustrated in Figure 1. In this figure, it can be observed that the dynamic model fails to compute the Smagorinsky constant when using either the FS or the FT methods as traditionally implemented. In this case the FT method strongly suppresses turbulence, resulting in the laminarization of the flow. Alternatively, while the consequences of using the FS method are less dramatic, the flow also exhibits a large acceleration at the top of the domain. As mentioned by the reviewer, these results are not surprising given that the dynamic models are using a relation between the small scales to compute the Smagorinsky constant. We believe that these could though be slightly improved by using information from scales larger than the traditional filtering scale, if the reader was really interested. Yet this reamins outside the scope of this manuscript. Therefore, it is advisable not to use the FT and FS methods with dynamic SGS

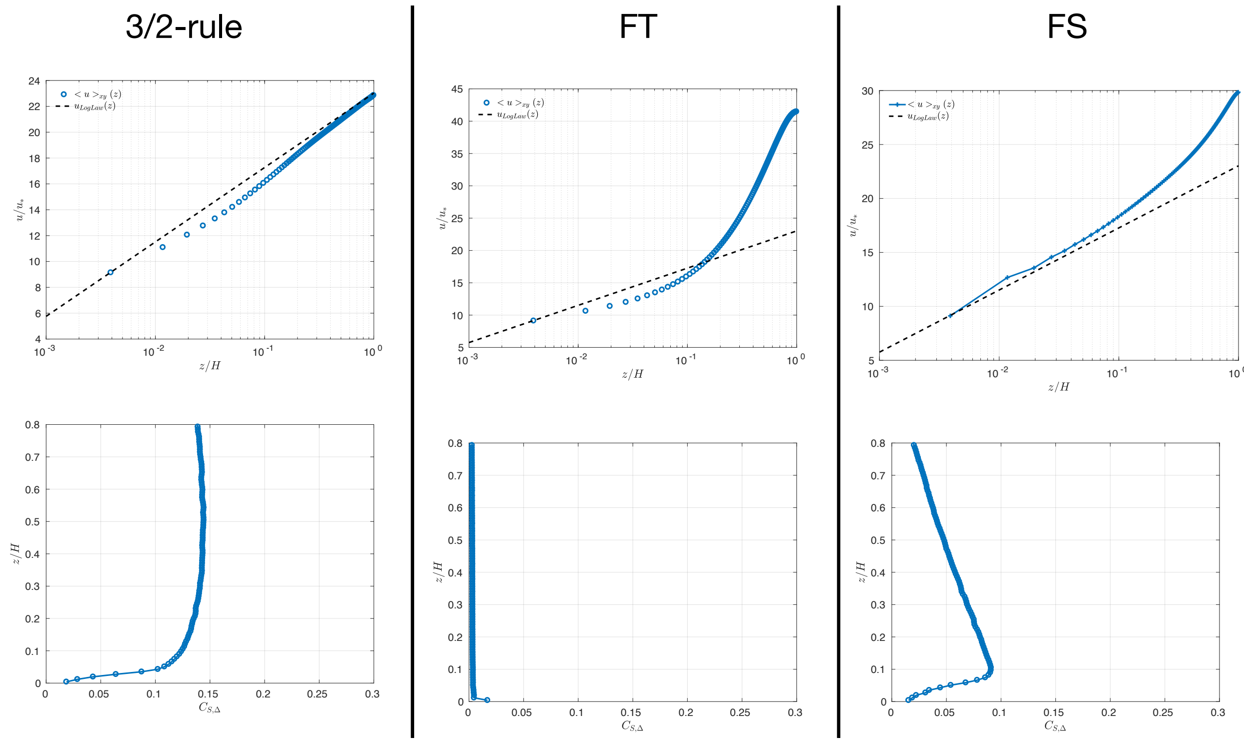

Figure 1: Profiles of the horizontal velocity and the Smagorinsky constant for the three deasliasing methods at a resolution of 128^3.

models. In this regard, we have added additional text in the new discussion section that relates to the use of dynamic models and the fact that they probably require some modification to run with the FT and FS methods.

Changes in manuscript: A discussion related to this comment has been added to the discussion section (see new discussion and conclusion section in comment #1).

3. **Reviewer comment:** *Fig 8d and the associate sentence "Interestingly, results of the vertical flux (or stress, resolved and SGS) of stream-wise momentum (figure 8(d)) illustrate a good agreement between the different scenarios." The authors should be careful in this interpretation. The constant pressure gradient forcing requires and forces the stress profile to be linear. Regardless of how turbulence ends up looking like the turbulent fluxes have to adjust to balance the mean $\partial P/\partial x$. What this figure indicates is that the SGS fraction is not strongly affected by the choice of dealiasing method, which is a good thing.*

   Authors response: Thank you for bringing this to our attention. As mentioned above the results section has been adjusted where this is taken care of.

4. **Reviewer comment:** *Figure 9, and more generally: I would have liked to see a direct comparison of*

the largest scales (by filtering all simulations at $n\Delta$, where n correspond to start of the damping or cutoff in figure 1) to see if the differences are only on the smallest scales or not (although given the mean velocity profiles, I suspect they are not).

Authors response: Thank you very much, this is a very interesting and important point. In order to answer this comment and clarify the effect of the FT and FS methods on the spectra, we have developed an additional analysis using the spectra presented in the paper. Although the effect of the FT and FS methods on the small scales can be clearly observed on the spectra, their effect on the large scales cannot be directly assessed from the figure, as pointed out by the reviewer. To compute a direct comparison scale by scale, the following ratio was used for the 128^3, 192^3, and 256^3-simulations,

$$\rho^{XX}(k) = \frac{E_{u,k}^{XX} - E_{u,k}^{3/2}}{E_{u,k}^{3/2}} \tag{1}$$

where $E_{u,k}$ denotes the power spectral density of the u velocity component at wavenumber k, XX stands for the dealiasing method FT or FS. Hence, if $\rho(k) < 0$ energy is removed at that scale, and if $\rho(k) > 0$ energy is added at that scale. Figure 2 presents the ratio $\rho(k)$ for both methods where it can be observed that the effect of FT methods is very large at all scales. The large scales ($0 \leq k/k_{max} \leq 0.2$) are affected with a reduction of energy of ∼25%. The mid-range scales ($0.2 \leq k/k_{max} \leq 0.6$), corresponding to the inertial sub-range, exhibit an overestimation of their energy of about ∼50% on average. Therefore, this method redistributes the energy of the small scales into the inertial sub-range scales. On the contrary, in the FS method, the energy from the filtered small-scales is redistributed more or less uniformly throughout with an averaged overall variation of less the 13%.

Changes in manuscript: We have added figure 2 and its interpretation in the manuscript. This now reads as: "Although the effect of the FT and FS methods on the small scale can be clearly observed in figure 9, their effect on the large scales also needs to be quantified. To compute a direct comparison scale by scale, the following ratio was used (equation 2) for the 128^3, 192^3, and 256^3-simulations,

$$\rho^{XX}(k) = \frac{E_{u,k}^{XX} - E_{u,k}^{3/2}}{E_{u,k}^{3/2}} \tag{2}$$

where $E_{u,k}$ denotes the power spectral density of the u velocity component at wavenumber k, XX stands for the dealiasing method FT or FS. If $\rho(k) < 0$ the energy density at that given wavenumber (k) is less than the corresponding one for the run using the $3/2$ rule, viceversa if $\rho(k) > 0$. Figure 2 presents the ratio $\rho(k)$ for both methods.

When using the FT method, energy at the low wavenumbers is underpredicted, whereas energy at the large wavenumbers is overpredicted. Departures are in general larger with decreasing resolution, with an excess of up to 100% for the 128^3-simulations in the wavenumber range close to the cutoff wavenumber. On the contrary, when using the FS method, the energy from the filtered (dealiased) small-scales is redistributed quasi-uniformly throughout the spectra with an averaged overall variation of less than 13%."

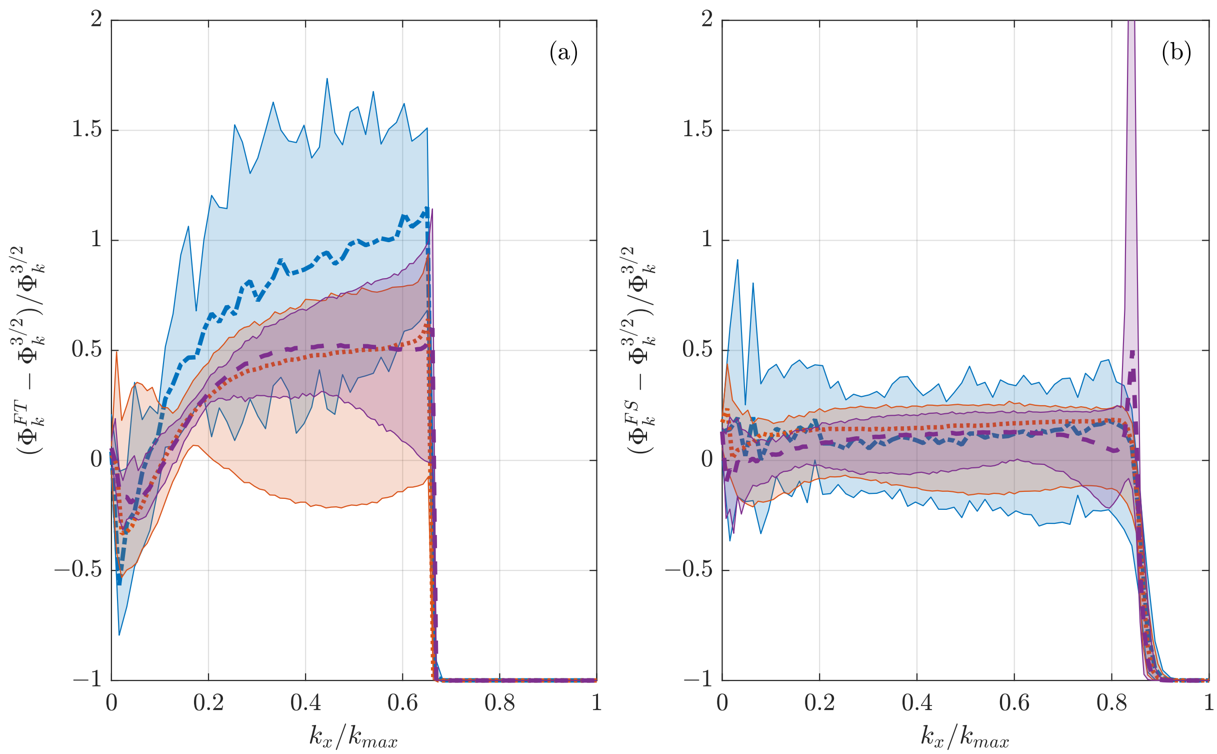

Figure 2: Effect of the FT (a), and the FS (b) methods of the stream-wise spectra of the stream-wise velocity compare to the 3/2-rule. The solid line represent the average value and the shaded area represent the extreme values. The resolutions are: 128^3 in blue dot-dashed line, 192^3 in red dotted line, and 256^3 in purple dashed line.

Minor comments:

1. **Reviewer comment:** *Title is long and too descriptive: how about replacing the wordy "atmospheric boundary- layer type flows" with "atmospheric flows". One in fact could foresee using such methods for cloud resolving LES outside the ABL. Same on last line of abstract: why restrict the applications only to ABL flows?*

   Authors response: Thank you for this comment. We have adapted these very interesting suggestions. The new title is included below, as well as the new abstract.

   Changes in manuscript: Title: "Comparison of dealiasing schemes in large-eddy simulation of neutrally-stratified atmospheric flows"

   Abstract: "Aliasing errors arise in the multiplication of partial sums, such as those encountered when numerically solving the Navier-Stokes equations, and can be detrimental to the accuracy of a numerical solution. In this work, a performance/cost analysis is proposed for widely-used dealiasing schemes in large-eddy simulation, focusing on a neutrally-stratified, pressure-driven atmospheric boundary-layer flow. Specifically, the exact 3/2 rule, the Fourier truncation method, and a high order Fourier smoothing method are inter-compared. Tests are performed within a newly developed mixed pseudo-spectral collocation - finite differences large-eddy simulation code, parallelized using a two-dimensional pencil decomposition. A series of simulations are performed at varying resolution and key flow statistics are inter-compared among the considered runs and dealiasing schemes. Both the Fourier Truncation and the Fourier Smoothing method correctly predict basic statistics. However, they both prove to provide less accurate flow statistics when compared to the traditional 3/2-rule. The accuracy of the methods is dependent of the resolution. The biggest advantage of both of these methods against the exact 3/2-rule is a notable reduction in computational cost with an overall reduction of 15% for a resolution of 128^3, 17% for 192^3 and 21% for 256^3."

2. **Reviewer comment:** *Abstract line 3: better to replace "integrating" by "time advancing"*

   Authors response: Thank you for pointing this out. The abstract has been significantly changed (see comment 1).

3. **Reviewer comment:** *Abstract lines 4-5: not sure what is meant by "This is of special relevance when using high order schemes." Spectral schemes are always "high order"*

   Authors response: Thank you. We realize that this sentence was miss-leading. In the manuscript, we were referring to the schemes used for the 3rd dimension and for the time advancement. The abstract has been significantly changed (see comment 1).

4. **Reviewer comment:** *First 3 lines (19-21) of introduction. In fact the # of grid points in LES has not been following Moores law. See https://doi.org/10.1017/jfm.2014.616 . This shows that the LES community has not been taking full advantage of increasing computing power to improve model accuracy, which I think is a remiss.*

   Authors response: Thank you for bringing this point to our attention.

   Changes in manuscript: We have added this comment in the introduction: "Despite this progress, high resolution simulations effectively exploiting current hardware and software capabilities (i.e., following Moore's law) are challenging as they require significant computational resources, which most research groups do not dispose of (Bou-Zeid, 2014). As a result, methods that aim at reducing computational requirements while preserving numerical accuracy are still of great interest."

5. **Reviewer comment:** *Page 2, line 2. Add comma after "With increasing computer power". I think there are a few other missing commas after introductory phrases.*

   Authors response: Thank you for pointing out these omissions. These have been amended.

6. **Reviewer comment:** *Correct wall bounded flow to wall-bounded flow on page 2 line 7.*

   Authors response: Thank you for pointing this out. This has been corrected.

7. **Reviewer comment:** *Page 2, Lines 30-32: authors talk about the need to expand the grid onto 3/2N and then say "As a result, due to the non-linear dependence on N" This example make it sound linear. I think they are referring to the non-linearity of the FFT cost with N, which they explain later. Clarify?*

   Authors response: Thank you for bringing this up. We realize that the sentence was confusing, and hence we have changed it in the text. In the manuscript, we are indeed referring to the cost of the FFT, given that the size of the expended grid is linear with N.

   Changes in manuscript: We have made the following modifications: "As a result, the computational burden introduced by these methods is high, mainly due to the non-linear increase of the cost of the fast Fourier transform algorithm (such as the one implemented in the FFTW library). Additionally, this cost rises more rapidly when the Fourier transform is performed in higher dimensions. Therefore, the treatment of aliasing errors severely limits the computational performances of large scale models based on high-order schemes."

8. **Reviewer comment:** *Also maybe they should clarify that if FFTs are used in 2D, the cost rises even more quickly as N rises.*

   Authors response: Thank you. We have clarified this point in the text (see comment 7)

9. **Reviewer comment:** *Page 3 line 5 "via a set of LES of fully developed ABL type flows and with a corresponding comparison on the effect in turbulent flow statistics and topology". Convoluted phrase. Simplify.*

   Authors response: Good point. We have simplified this phrase.

   Changes in manuscript: It now reads as: "In this work, we provide a cost-benefit analysis and a comparison of turbulent flow statistics for the FT and FS dealiasing schemes in comparison to the exact 3/2-rule using a set of LES of fully developed ABL type flows."

10. **Reviewer comment:** *Page 3, line 8 "environmental fluids"*

    Authors response: Thank you for pointing out the misspelling.

11. **Reviewer comment:** *Page 4, line 19 "thus discouraging its use in most practical situations" are the authors certain of this statement? The 3/2 rule is use very very widely. If not maybe their paper would be a good reference for modelers to see the advantages of using it.*

    Authors response: In this sentence we were originally referring to the phase shift method not to the 3/2 rule. We are well aware that the 3/2-rule is widely used. In this regard we realize that the text was not very clear, and hence we have rewritten the sentence.

    Changes in manuscript: It now reads as: "This method has a cost equal to $15N\log_2(N)$ (Canuto et al., 2006), which is even greater than the 3/2-rule (Patterson, 1971; Orszag, 1972), discouraging its use in most practical situations."

12. **Reviewer comment:** *Page 5 line 13, and maybe other places. Referring to the production range as the energy containing range is inaccurate and misleading. The statement "For this technique to be successful, the low-pass filter operation must be performed at a scale smaller than the smallest energy containing scale, deep in the inertial sub-range according to Kolmogorovs hypothesis (Kolmogorov, 1968; Piomelli, 1999)." For example makes no sense if that jargon is used. Please fix and use energy production range instead.*

    Authors response: Thanks, this is a very good point. In this regard we have revised the manuscript and changed this reference for '*energy production range*' as indicated by the reviewer.

13. **Reviewer comment:** *Eq 8, the τ should have a d superscript if the trace is already in $p*$ as the authors write.*

    Authors response: Thank you for pointing this out. This has been corrected.

14. **Reviewer comment:** *Page 6, line 18: the log law is not inviscid since it is derived from matching the viscous sublayer and the outer layer. If the wall is smooth for example z_0 depends on viscosity.*

    Authors response: Thank you for pointing this out. We have modified the text to avoid the miss-understanding.

Changes in manuscript: The text now reads as: "Note that the molecular viscous term has been neglected within the flow. However, the effect of the molecular viscosity at the surface is modeled using the logarithmic law, where the surface drag is parameterized through the surface roughness."

15. **Reviewer comment:** *Page 6 line 25: what does "module" mean? Do they mean modulus?*

    Authors response: Indeed. We have clarified this in the manuscript.

16. **Reviewer comment:** *Should equation 12 include f_i to be consistent ?*

    Authors response: Thanks, this has been corrected.

17. **Reviewer comment:** *Page 8, lines 10-15: Authors should clarify this is with the baseline 3/2 dealiasing I presume. Also how does the parallelization method impact these numbers?*

    Authors response: Thank you for pointing this out, we used the 3/2 as a baseline. In addition, an other comment on this regard was also made by an other reviewer, and hence we have included some clarification in the manuscript.

    Here is our response to the question regarding the parallelization and the pressure solver. We have noticed that the cost breakdown for the resolution of the convective term and the Poisson solver is also influenced by the pencil decomposition.

    When treating the convective term with the pencil decomposition, the communication cost increases with respect to the traditional slice parallelization. In this case, a total of nine transpositions are needed to compute the convective term, significantly increasing the computational cost.

    Opposite, the Poisson solver becomes faster when using the pencil decomposition in comparison to the slice parallelization. Note that in the pseudo-spectral method the horizontal directions (x and y) are treated in Fourier space and only the vertical direction (z) remains in physical space, therefore each mode in k_x and k_y become independent of each other. In this case the system of equations, originally of size $n_x \times n_y \times n_z$ becomes $n_x \times n_y$ systems of n_z equations, making each vertical line in the domain independent. The pencil decomposition can take full advantage of this fact, making the resolution of the Poisson equation faster. Specifically, once the domain is transposed in the Z-pencil (square pipe aligned with the z-coordinate), the process of solving each of the $n_x \times n_y$ systems does not require any communication, making it very efficient, and limiting its cost to the transposition between the different pencils.

    Changes in manuscript: We realize that this is an important detail that should be also mentioned in the manuscript. For this reason we have included a couple of lines in section 3.3.

    The text now reads as: "In addition, it is important to note that the low computational cost of the Poisson solver is related to the the use of the pencil decomposition, which takes full advantage the pseudo-spectral approach. Specifically, the Z-pencil combines with the horizontal treatment of the derivatives to make the implementation of the solver very efficient."

18. **Reviewer comment:** *Page 10, lines 1-2: The z_0 they impose is 1cm, which corresponds more to a grass field than to a sparse forest of to a farmland. I suggest they check Brutsaerts books rather than to Stull for z_0.*

Authors response: We realized that there was a mistake in the actual value of z_0. This one is actually of 0.1m, which corresponds to a sparse forest according to Stull and Brutsaert. We added the reference to Brutsaert's book in the manuscript.

19. **Reviewer comment:** *Figure 5 and other are difficult to read. Why not use colors for the online version (Color is free with EGU, no?)*

    Authors response: Because we couldn't find any information in this regard on the publisher web page we decided to go on black & white. If the editor confirms that color figures are free of charge, then we would be happy to change them

20. **Reviewer comment:** *Page 11, lines 9-11: 30% drop in the convective term cost is good but I would not say it is significant. It would only be equivalent to about 20% drop in total computing time (given Fig 2), which would only be equivalent to a 5% reduction in the resolution. So I would remove significantly on line 9.*

    Authors response: We have removed the "significantly" in the text. Additional detail in this regard has been provided earlier in comment 17.

21. **Reviewer comment:** *Page 11, lines 10-11: "the predicted computational cost predicted by" remove one of the "predicted".*

    Authors response: Thank you for pointing out the repetition.

22. **Reviewer comment:** *Page12, line 2: replace "extend" with "extent"*

    Authors response: Thank you for pointing out the misspelling.

23. **Reviewer comment:** *Page12, line 9: correct the misspelling of "stream-wise"*

    Authors response: Thank you for pointing out the misspelling.

24. **Reviewer comment:** *Page 12 line 25, and page 14 line 10: "differentiated" is an unclear word. Please remove and clarify the two sentences.*

    Authors response: Thank you for pointing out these two sentences. The discussion of the results have been changed and these sentences have been removed.

25. **Reviewer comment:** *Page 14 lines 15-16. There wont be any dispersive stresses in their simulations over homogeneous terrain so why mention them?*

    Authors response: In order to avoid any confusion in the discussion, we remove the mention to dispersive stresses in the text

Comparison of dealiasing schemes in large-eddy simulation of neutrally-stratified atmospheric ~~boundary-layer type~~ flows

Fabien Margairaz[1], Marco G. Giometto[2], Marc B. Parlange[3], and Marc Calaf[1]

[1]University of Utah, Department of Mechanical Engineering, 1495 E 100 S, Salt Lake City, Utah 84112, USA
[2]Columbia University, Civil Engineering and Engineering Mechanics, 500 W. 120th St., 610 Mudd, New York, NY 10027, USA
[3]Monash University, Department of Civil Engineering, Scenic Blvd, Clayton VIC 3800, Australia

Correspondence to: Marc Calaf (marc.calaf@utah.edu)

Abstract. ~~Three dealiasing schemes for large-eddy simulation of turbulent flows are inter-compared for the canonical case of pressure-drive atmospheric boundary-layer type flows.~~ Aliasing errors arise in the multiplication of partial sums, such as those encountered when ~~integrating the non-linear terms of the~~ numerically solving the Navier-Stokes equations~~in spectral methods (Fourier or polynomial discrete series), and are~~ , and can be detrimental to the accuracy of ~~the~~ a numerical solution. ~~This is of special relevance when using high-order schemes.~~ In this work, a performance/cost analysis is ~~developed for three well-accepted approaches:~~ proposed for widely-used dealiasing schemes in large-eddy simulation, focusing on a neutrally-stratified, pressure-driven atmospheric boundary-layer flow. Specifically, the exact 3/2 rule, the Fourier truncation method, and a high order Fourier smoothing method ~~.~~ are inter-compared. Tests are performed within a newly developed mixed pseudo-spectral collocation - finite differences large-eddy simulation code, parallelized using a two-dimensional pencil decomposition. ~~The static Smagorinsky eddy-viscosity model with wall damping of the model coefficient is used.~~ A series of simulations are performed at varying resolution and key flow statistics are inter-compared among the considered runs and dealiasing schemes. ~~The numerical results validate the numerical performance predicted by theory when using the Fourier truncation and Fourier smoothing methods. In terms of turbulence statistics, the Fourier Truncation method proves to be over-dissipative when compared against the Fourier Smoothing method and the~~ Both the Fourier Truncation and the Fourier Smoothing method correctly predict basic statistics. However, they both prove to provide less accurate flow statistics when compared to the traditional 3/2-rule~~, leading to an enhanced horizontal integrated mass flux and to higher dispersive momentum fluxes. Its use in large-eddy simulation of atmospheric boundary-layer type flows is therefore not recommended. Conversely, the Fourier Smoothing method yields accurate flow statistics, comparable to those resulting from the application of the~~ . The accuracy of the methods is dependent of the resolution. The biggest advantage of both of these methods against the exact 3/~~2 rule, with a significant~~ 2-rule is a notable reduction in computational cost ~~, which makes it a convenient alternative for use in the studies related to the atmospheric boundary layer~~with an overall reduction of 15% for a resolution of 128^3, 17% for 192^3 and 21% for 256^3.

1 Introduction

The past decades have seen significant progress in computer hardware in remarkable agreement with Moore's law, which states that the number of nodes in the discretization grids ~~double~~ doubles every eighteen months (Moore, 1965; Voller and Porté-Agel, 2002; Takahashi, 2005). A comparable progress has been made in software development, with the rise of new branches in numerical analysis like reduced order modeling (Burkardt et al., 2006) and uncertainty quantification (Najm, 2009), as well as the development of highly efficient numerical algorithms and computing frameworks like Isogeometric Analysis (Hsu et al., 2011) or GPU-computing (Hamada et al., 2009; Bernaschi et al., 2010) ~~. With~~

At the same time, with increasing computer power, the range of scales and applications in computational fluid dynamics (CFD) has significantly broadened, allowing to describe at an unprecedented level of detail complex flow systems such as fluid-structure interaction (Hughes et al., 2005; Bernaschi et al., 2010; Takizawa and Tezduyar, 2011), land-atmosphere exchange of scalars, momentum and mass ~~(Moeng, 1984; Bou-Zeid et al., 2004; Tseng et al., 2006; Calaf et al., 2010; Anderson et al., 2012; Giometto~~ weather research and forecasting (Skamarock et al., 2008), micro-fluidics (Wörner, 2012), and canonical ~~wall bounded~~ wall-bounded flows (Schlatter and Örlü, 2012), to name but a few. Despite this progress, ~~very high Reynolds number flows – such as those characterizing the atmospheric boundary layer (ABL) – still remain challenging with the cost of full resolution numerical simulations remaining out of reach~~high resolution simulations effectively exploiting current hardware and software capabilities (i.e., following Moore's law) are challenging as they require significant computational resources, which most research groups do not dispose of (Bou-Zeid, 2014). As a result, methods that aim at reducing computational requirements while preserving numerical accuracy are still of great interest.

The Fourier-based pseudo-spectral collocation method (Orszag, 1970; Orszag and Pao, 1975; Canuto et al., 2006) remains the preferred "work-horse" in simulations of wall-bounded flows over ~~horizontally periodic~~ horizontally-periodic regular domains. This is often used in conjunction with a centered finite-difference or Chebychev polynomial expansions in the vertical direction ~~(Shah and Bou-Zeid, 2014; Moeng and Sullivan, 2015)~~(Albertson, 1996; Moeng and Sullivan, 2015). The main strength of such an approach is the high-order of accuracy of the Fourier partial sum representation, coupled with the intrinsic efficiency of the fast-Fourier-transform algorithm (Cooley and Tukey, 1965; Frigo and Johnson, 2005). In such algorithms the leading order error term is represented by the aliasing that arises when evaluating the quadratic non-linear term (convective fluxes of momentum). This was first discovered in the early works of Orszag and Patterson (Orszag, 1971; Patterson, 1971) which also set a cornerstone in the treatment and removal of aliasing errors in pseudo-spectral collocation methods. Aliasing errors can severely deteriorate the quality of the solution, as exemplified by the large body of literature that has dealt with the topic. In Horiuti (1987) and Moin and Kim (1982), it was shown how the energy-conserving rotational form of the Large-Eddy ~~Simulation~~ simulation (LES) equations performed poorly without dealiasing, and that proper removal of such error significantly improved the accuracy of the solution on statistics like the flow turbulent shear stress, turbulence intensities and two point correlations. As shown in Moser et al. (1983); Zang (1991); Kravchenko and Moin (1997), aliasing errors do not alter the energy conservation properties of the rotational form of the LES equations, but the additional dissipation that is introduced makes the flow prone to laminarization. Dealiasing is hence required in order to accurately resolve turbulent flows with a well developed inertial ~~subrange~~sub-range, such as ABL flows for instance. However, the classic (exact) dealiasing methods developed in (Patterson, 1971) based on padding and truncation (the 3/2 rule) or on the phase-shift technique, have proven to be computationally expensive, and are one of the most costly module for momentum integration in high resolution simulations, as it will be shown later in this work. For example, in simulations with Cartesian discretization, where N is the number of collocation nodes in each of the three coordinate directions, the 3/2 rule requires to expand the number of nodes to $3/2 \times N$, and the phase-shift method needs grids with $2 \times N$ nodes. As a result, ~~due to the non-linear dependence on N, the~~ the computational burden introduced by ~~such~~ these methods is high, ~~and increases with increasing grid resolution, thus severely limiting computational performances in~~ mainly due to the non-linear increase of the cost of the fast Fourier transform algorithm (such as the one implemented in the FFTW library). Additionally, this cost rises more rapidly when the Fourier transform is performed in higher dimensions. Therefore, the treatment of aliasing errors severely limits the computational performances of large scale models ~~.~~ based on high-order schemes.

This has motivated efforts towards the development of approximate yet computationally efficient dealiasing schemes, such as the Fourier truncation (FT) method ~~(Orszag, 1971; Moeng, 1984; Moeng and Wyngaard, 1988; Albertson, 1996)~~(Orszag, 1971; Moeng, 19 the Fourier smoothing (FS) method (Hou and Li, 2007), and the more recent implicit dealiasing of Bowman et al. (Bowman and Roberts, 2011). Details on the FT and the FS techniques are provided in the following section. Limits and merits of the different dealiasing techniques have been extensively discussed in the past decades within the turbulent flow framework (Moser et al., 1983; Zang, 1991).

In this work, we provide a cost-benefit analysis and a comparison of turbulent flow statistics for the FT and FS dealiasing schemes in comparison to the exact ~~3/2-rule, via~~ 3/2-rule using a set of LES of fully developed ABL type flows~~and with a corresponding comparison on the effect in turbulent flow statistics and topology~~. Simulations and benchmark ~~analyses~~ analysis are performed using a recently-developed mixed pseudo-spectral finite difference code~~parallelized using~~ , parallelized via a pencil decomposition technique based on the 2DECOMP&FFT library (Li and Laizet, 2010). Results of this work are of prime interest to the environmental ~~fluid~~ fluids community (e.g. ABL community) because they can help improve the numerical performance of some of the numerical approaches used. An overview on the different dealiasing methods is provided in section 2. Section 3 briefly presents the LES platform with important benchmark results. The computational cost analysis and flow statistics obtained with the different dealiasing schemes are later discussed in section 4. Finally, the conclusions are presented in section 6.

2 Dealiasing methods

Aliasing errors result from representing the product of two or more variables by N wave-numbers, when each one of the variables is itself represented by a finite sum of N terms (Canuto et al., 2006), here N is assumed even. Such is the case for example when treating the non-linear advection term in the Navier-Stokes (NS) equations. Let f and g be two smooth functions with the corresponding discrete Fourier transforms expressed as,

$$f(x) = \sum_{k=-N/2}^{N/2-1} \hat{f}_k e^{ikx} \quad \text{and} \quad g(x) = \sum_{m=-N/2}^{N/2-1} \hat{g}_k e^{ikx}, \tag{1}$$

with $\hat{f}_k$ and $\hat{g}_k$ being the amplitudes of the k-th Fourier mode of f and g. The product of the two functions is hence given by

$$h(x) = f(x)g(x) = \sum_{m=-N/2}^{N/2-1} \hat{f}_m e^{imx} \sum_{n=-N/2}^{N/2-1} \hat{g}_n e^{inx} = \sum_{k=-N}^{N-1} \hat{h}_k e^{ikx}, \tag{2}$$

with

$$\hat{h}_k = \sum_{m+n=k} \hat{f}_n \hat{g}_m \quad \text{and } |m|,|n| \leq N/2. \tag{3}$$

Note that the corresponding expression for the Fourier transform of the product h (result of the convolution of f with g) requires $2N$ modes. Therefore, the exact computation of the product represents a major numerical cost. Traditionally the convolution of the two functions f and g is made with only N Fourier modes,

$$h(x) = \sum_{k=-N/2}^{N/2-1} \tilde{h}_k e^{ikx}. \tag{4}$$

As a result, the energy contained within the remaining $N+1$ to $2N$ modes folds back on the first N modes, and the amplitude of the first N modes ($\tilde{h}_k$) is aliased. This can be related to the exact amplitude $\hat{h}_k$ as,

$$\hat{h}_k = \sum_{m+n=k} \hat{f}_n \hat{g}_m + \sum_{m+n=k\pm N} \hat{f}_n \hat{g}_m = \tilde{h}_k + \sum_{m+n=k\pm N} \hat{f}_n \hat{g}_m, \tag{5}$$

with

$$\tilde{h}_k = \sum_{m+n=k} \hat{f}_n \hat{g}_m \quad \text{and } -N/2 \leq k \leq N/2-1, \tag{6}$$

such that the second term contains the aliasing errors on the k-th mode. Aliasing errors propagate in the solution of the differential equation and can induce large errors. For the pseudo-spectral methods, the truncation and aliasing errors affect both the accuracy and the stability of the numerical solution (see (Canuto et al., 2006) chap. 3 and (Canuto et al., 2007) chap. 3 for detailed discussion). Traditionally, the aliasing errors are treated using one of the two methods discussed below.

The 3/2 rule method is based on the so-called padding and truncation technique, where the Fourier partial sums are zero-padded in Fourier space by half the available modes (from N to $3/2N$), inverse-transformed to physical space before multiplication, multiplied, and then truncated back to the original variable size (N). This method fully removes aliasing errors. However, the high computational cost related to the inverse transform operation discourages its use in large scale simulations~~as the~~. The fast Fourier transform (FFT) algorithm has an operational complexity of $N\log_2(N)$~~. Thus,~~; counting the number of FFT and multiplications, the operation count of the 3/2-rule applied to dealias the product of two vectors of N

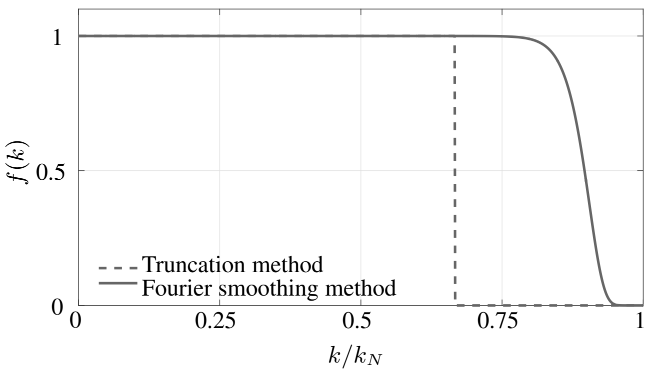

Figure 1. Weighting functions used in the FT method (dashed kine) and the FS method (continuous line). The FT method filters scales with $k/k_N > 2/3$ and the FS method at $k/k_N > 3/4$.

components becomes $(45/4)N\log_2(3N/2)$ (Canuto et al., 2006). An alternative method is the so-called Phase Shift method which consists in shifting the grid of one of the variables in physical space. Given the appropriate shift, the aliasing errors are eliminated naturally in the evaluation of the convolution sum. This method ~~, however,~~ has a cost equal to $15N\log_2(N)$ (Canuto et al., 2006), which is even greater than the 3/2-rule (Patterson, 1971; Orszag, 1972)~~, thus discouraging its use in most practical situations~~. The discussion above concerns one dimensional problems but the expansion to higher dimensional problems is straightforward (Iovieno et al., 2001; Canuto et al., 2006). Although, this method provides the full dealiasing of the non-linear term, the cost of expanding the number of Fourier modes by a factor of $3/2$ is a computationally expensive endeavour, especially with the progressive increasing size of numerical grids. To reduce the numerical burden, two additional methods were proposed in the past for treating the aliasing errors: the FS method (Hou and Li, 2007), and the FT method ~~(Orszag, 1971; ?)~~(Orszag, 1971; Moeng, 1984; Moeng and Wyngaard, 1988). In both methods, a set of high-wave-number Fourier amplitudes are multiplied by a test function $\hat{u}_k^* = f(k)u_k$, to avoid expansions to larger number of modes. As its name indicates, the FT method sets to zero the last third of the Fourier modes ($f(k) = 0$, for $k > 2N/3$), ~~similar~~ equivalent to a sharp spectral cut-off filter. On the other hand, the FS method consists on a progressive attenuation of the higher frequencies using the weighting function $f(k) = e^{-36k^{36}}$ (Hou and Li, 2007). Figure 1 presents the spectral function $f(k)$ for the two different methods. Note that both the FT and FS methods behave like a low-pass filter. Although the FT method (continuous line) sets to zero any coefficient larger than $k/k_N > 2/3$, the FS method (dashed line) keeps all the wavelengths unperturbed up until $k/k_N > 3/4$, and then progressively damps the amplitude of the higher wave-number terms. The advantage of both of these methods is that they avoid the need for padding the Fourier partial sums, and hence reduce the numerical cost. Specifically, the computational cost of these methods is ~~$(15/2)N^3\log_2(N)$~~ $(15/2)N\log_2(N)$ (Canuto et al., 2006), resulting in methods 33% less computationally expensive than the 3/2-rule. The drawback of such approximate approaches is however the fact that a filtering operation is applied to the advection term, resulting in a loss of information. A desirable property of the FS technique when compared to the FT method is that the former exhibits a more localized error and is dynamically very stable (Hou and Li, 2007), while the latter tends to generate oscillations on the whole domain.

3 Large-eddy simulation framework

3.1 Equations and boundary conditions

The LES approach consists of solving the filtered NS equations, where the time- and space-evolution of the turbulent eddies larger than the grid size are fully resolved, and the effect of the smaller ones is parametrized. Mathematically, this is described through the use of a numerical filter that separates the larger, energy containing eddies from the smaller ones. Often, the numerical grid of size Δ is implicitly used as a top-hat filter, hence reducing the computational cost (Sagaut (2006), see Moeng and Sullivan (2015) for an overview of the technique in ABL research). As a result, the velocity field can be separated in a resolved component ($\tilde{u}_i$, where $i = 1,2,3$) and an unresolved contribution (u_i') (Smagorinsky, 1963). For this technique to be successful, the low-pass filter operation must be performed at a scale smaller than the ~~smallest energy containing scale~~energy production range, deep in the inertial sub-range according to Kolmogorov's hypothesis (Kolmogorov, 1968; Piomelli, 1999). In atmospheric boundary-layer flow simulations this requirement is known to hold in the bulk of the flow, where contributions from the Sub-Grid Scale (SGS) motions model (or sub-filter scale motions) to the overall dissipation rate are modest. In the near surface regions such requirement is not met, as the characteristic scale of ~~energy-containing motions~~ the energy production range $\mathcal{L}$ scales with the distance from the wall ($\mathcal{L} \approx \kappa z$, where $\kappa \approx 0.4$ is the Von Kármán constant, and z is the wall-normal distance from the wall), hence remaining an active research field (Sullivan et al., 1994; Meneveau et al., 1996; Porté-Agel et al., 2000; Hultmark et al., 2013; Lu and Porté-Agel, 2014). In this work, the rotational form of the filtered NS equations are integrated, ensuring conservation of mass of the inertial terms (Kravchenko and Moin, 1997). The corresponding dimensional form of the equation reads as

$$\partial_i \tilde{u}_i = 0, \tag{7}$$

$$\partial_t \tilde{u}_i + \tilde{u}_j \left(\partial_j \tilde{u}_i - \partial_i \tilde{u}_j\right) = -\partial_i \tilde{p*} - \partial_j \cancel{\tau^{\Delta}_{ij}}\,\tau^{\Delta,d}_{ij} + \tilde{f}_i. \tag{8}$$

In these equations, $\tilde{u}_i$ are the velocity components in the three coordinate directions x, y, z (~~stream-wise, span-wise~~streamwise, spanwise, and vertical respectively), $\tilde{p}^*$ denotes the perturbed modified pressure field defined as $\tilde{p}^* = \tilde{p} + \frac{1}{3}\rho_0 \tau^{\Delta}_{kk} + \frac{1}{2}\tilde{u}_j\tilde{u}_j$, where the first term is the kinematic pressure, the second term is the trace of the sub-grid stress tensor and the last term is an extra term coming from the rotational form of the momentum equation. Here, $\tilde{f}_i$ represents a generic volumetric force. The flow is driven by a constant pressure gradient in the ~~stream-wise~~ streamwise direction imposed through the body force $\tilde{f}_i$. The sub-grid stress tensor is defined as $\tau^{\Delta}_{ij} = \widetilde{u_i u_j} - \tilde{u}_i\tilde{u}_j$, where the deviatoric components are written using an eddy-viscosity approach

$$\tau^{\Delta,d}_{ij} = \tau^{\Delta}_{ij} - \frac{1}{3}\tau^{\Delta}_{kk}\delta_{ij} = 2\nu_T \tilde{S}_{ij}, \tag{9}$$

with $\nu_T = (C_S\Delta)^2|\tilde{S}|$ being the so-called eddy-viscosity, $\tilde{S}_{ij} = \frac{1}{2}\left(\partial_j \tilde{u}_i + \partial_i \tilde{u}_j\right)$ the resolved strain rate tensor, and C_S the Smagorinsky coefficient, a dimensionless proportionality constant (Smagorinsky, 1963; Lilly, 1967). Many studies have investigated the accuracy of this type of models, showing good behaviour for free-shear flows (Lesieur and Metais, 1996). For boundary layer flows, the Smagorinsky constant model is over-dissipative close to the wall, since the integral length-scale scales with the distance to the wall. Therefore, to properly capture the dynamics close to the surface, the Mason-Thompson damping wall function is used (Mason, 1994). This function is given by $f(z) = (C_o^n(\kappa z)^{-n} + \Delta^{-n})^{-\frac{1}{n}}$, and is used to decrease the value of C_S close to the wall, reducing the sub-grid dissipation.

Note that the molecular viscous term has been neglected ~~, consistent with the idea of flow over fully rough surfaces, whose drag is parameterized via the inviscid logarithmic equilibrium law assumption (see below).~~ in the governing equations, including the wall-layer parameterization, which is equivalent to assuming that the surface drag is mostly caused by pressure (i.e., there are negligible viscous contributions). This is a typical situation in flow over natural surfaces where the surface is often in fully rough aerodynamic regime.

The drag from the underlying surface is entirely modeled in this application through the equilibrium logarithmic law for rough surfaces (Kármán, 1931; Prandtl, 1932), with

$$\tau_W = \left[\frac{\kappa}{\log(\Delta z/2z_0)}\right]^2 \left(\langle\tilde{u}_1\rangle^2(\Delta z/2) + \langle\tilde{u}_2\rangle^2(\Delta z/2)\right). \tag{10}$$

In equation (10), $\langle\tilde{u}_i\rangle$ is the planar averaged velocity sampled at $\Delta z/2$, z_0 is the ~~hydrodynamic~~ aerodynamic roughness length, representative of the underlying surface, Δz denotes the vertical grid stencil, and ~~$\kappa = 0.41$~~ $\kappa = 0.4$ is the von Kármán constant. The wall shear-stress is computed considering the ~~module~~ norm of the horizontal velocity and it is projected over the horizontal directions using the unit vector n_i, such that $\tau_{W,i} = \tau_W \, n_i$, where

$$n_i = \frac{\langle\tilde{u}_i\rangle(\Delta z/2)}{\sqrt{\langle\tilde{u}_1\rangle^2(\Delta z/2) + \langle\tilde{u}_2\rangle^2(\Delta z/2)}}, \text{ for } i = 1, 2. \tag{11}$$

In addition, the corresponding vertical derivatives of the horizontal mean velocity field are imposed at the first grid point of the vertically staggered grid ~~(Albertson et al., 1995; ?)~~(Albertson et al., 1995; Albertson and Parlange, 1999).

This setup has now been extensively used to study neutrally stratified ABL flows (Cassiani et al., 2008; Brasseur and Wei, 2010; Abkar and Porté-Agel, 2014; Allaerts and Meyers, 2017). Moreover, it is used as foundation to build more complex simulation of the ABL adding scalar (passive or active) transport (for example, see Saiki et al. (2000), Stoll and Porté-Agel (2008), Calaf et al. (2011), or Salesky et al. (2016)), and many more.

3.2 Numerical implementation and time integration scheme

The equations are solved using a pseudo-spectral approach, where the horizontal derivatives are computed using discrete Fourier transforms and the vertical derivatives are computed using second order-accurate centered finite differences on a staggered grid. A projection fractional-step method is used for time integration following Chorin's method (Chorin, 1967, 1968). The governing equations become decoupled and the system of partial differential equations can be solved in two steps: at first, the non-linear advection-diffusion equation is explicitly advanced, and subsequently the Poisson equation is integrated (the so-called pressure correction step). The latter equation is obtained by taking the divergence of the first equation and setting the divergence of velocity at the next time step equal to zero, to ensure a divergence free flow field. The algorithm is detailed in the rest of the section. Initially, the code computes the velocity tensor $\tilde{G}_{ij}^t = \partial_j \tilde{u_i}^t$, which contains all the derivatives of the flow

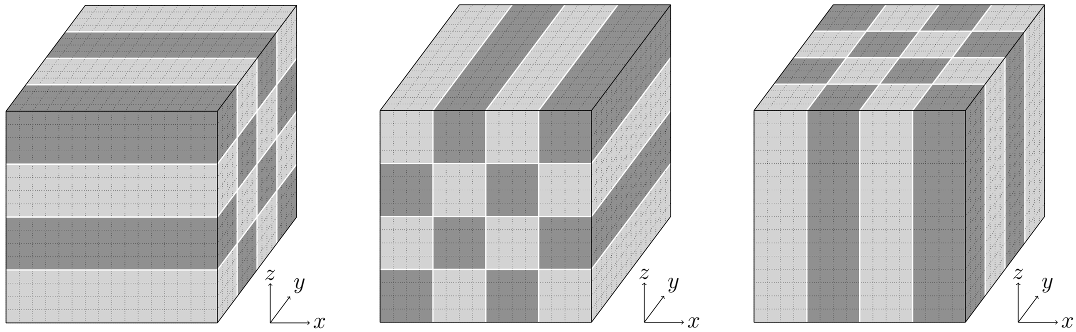

(a) (b) (c)

Figure 2. 2D Pencil decomposition of the computational domain with the domain transposed into the 3 direction of space: (a) X-pencil, (b) Y-pencil, (c) Z-pencil (inspired form (Li and Laizet, 2010)).

field required to compute the SGS stress tensor $\cancel{\tau_{ij}^{\Delta,t} = -2(C_S\Delta)^2|\tilde{S}^t|\tilde{S}^t_{ij}}\tau_{ij}^{\Delta,d,t} = -2(C_S\Delta)^2|\tilde{S}^t|\tilde{S}^t_{ij}$. In the first step of the projection method, the NS equations are solved without the pressure. Hence, the intermediary right hand side is computed as

$$\widetilde{RHS}_i^* = \left[\tilde{u_j}^t\left(\partial_j\tilde{u_i}^t - \partial_i\tilde{u_j}^t\right) - \partial_j\tau_{ij}^{\Delta,t}{}_j\tau_{ij}^{\Delta,d,t} + \tilde{f}_i\right]. \tag{12}$$

Next, an intermediary step is computed using an Adams-Bashforth scheme, following

$$\tilde{u}_i^* = u_i^t + \Delta t\left(\frac{3}{2}\widetilde{RHS}_i^* - \frac{1}{2}\widetilde{RHS}_i^{t-\Delta t}\right), \tag{13}$$

where $\widetilde{RHS}_i^{t-\Delta t}$ is the right hand side of the previous step. At this point, the resulting flow field is not divergence free yet. The modified pressure is used to impose this fundamental property of the flow filed. Therefore, $\tilde{p^*}^t$ is computed solving the Poisson equation

$$\partial_j\partial_j\tilde{p^*}^t = \partial_k\Gamma_k^t, \tag{14}$$

obtained by taking the divergence of the NS equations. The term Γ_k^t in the right hand side of the equation above is given by

$$\Gamma_k^t = \left(\frac{2}{3\Delta t}\right)\tilde{u}_k^t - \frac{1}{3}\widetilde{RHS}_k^{t-\Delta t}. \tag{15}$$

The new flow field for the complete time step is obtained by $\tilde{u}_i^t = \tilde{u}_i^* - \frac{3}{2}\Delta t\partial_i\tilde{p^*}^t$. Finally, the new right hand side is updated with the pressure gradient as $\widetilde{RHS}_i^{t+\Delta t} = \widetilde{RHS}_i^* - \partial_i\tilde{p^*}^t$.

Embedded within this approach, periodic boundary conditions are imposed on the horizontal (x,y) directions. To close the system, a stress free lid boundary condition is imposed at the top of the domain and an impermeability $(\tilde{w}=0)$ condition is imposed at the lower boundary, which sums to the parametrized stress described in section 3.

~~For time-integration performance, the~~ The code is parallelized following a 2D pencil decomposition paradigm similar to the one presented in Sullivan and Patton (2011), partitioning the domain into squared cylinders aligned along one of the

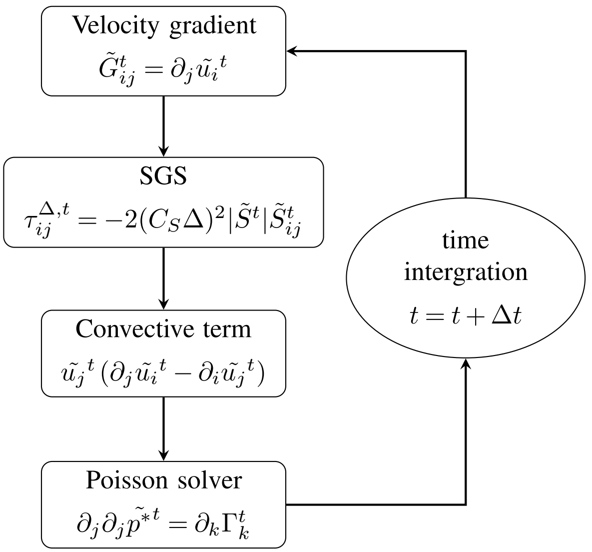

Figure 3. Simplified flowchart of the main algorithm presenting the four modules that represent the bulk of the computational cost.

horizontal directions, as shown in figure 2. ~~This parallelization scheme allows bigger computational domains when compared to the layer-based 'z-slice' decomposition schemes (Kumar et al., 2006; Kumar, 2007), where the domain was only split in horizontal slices.~~ The 2D ~~stencil~~ pencil decomposition is implemented using the 2DECOMP & FFT open source library (Li and Laizet, 2010), which shows exceptional scalability up to a large number of MPI processes (Margairaz et al., 2017).

3.3 Analysis of the numerical cost

The LES algorithm can be separated into four distinct modules: (1) computation of the velocity gradients, (2) evaluation of the SGS stresses and (3) of the convective term, and (4) computation of the pressure field by solving the Poisson equation. These four modules represent the bulk of the computational cost of the code, in addition to MPI communication. Figure 3 presents a simplified flowchart of the main algorithm with each of the four modules.

The four modules have been individually timed to evaluate their corresponding computational cost at a resolution of $N_x \times N_y \times N_z = 128^3$ with the 3/2-rule as a baseline. Results are shown in figure 4. As it can be observed, more than half of the integration time step ($\sim 60\%$) is spent computing the convective term. The three other modules share the rest of the integration time as follows: the computation of the velocity gradients ($\sim 20\%$), the Poisson solver ($\sim 16\%$) and the SGS ($\sim 4\%$). It is important to note that this test was conducted without any I/O as it is not relevant to assess the computational cost of the momentum integration. As explained in section 2, the non-linear term requires the use of dealiasing techniques to control the aliasing error, which traditionally are associated with a padding operation (as mentioned in Section 2), and hence higher computational cost. It is important to note that although the overall integration time distribution between each individual module might vary depending on the numerical resolution employed~~(*i.e.* the cost of the Poisson solver is expected~~

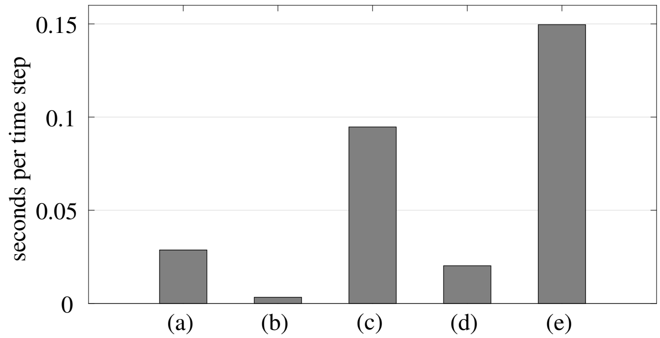

Figure 4. Individual timing of the 4 modules of the time loop averaged over 10k steps: (a) velocity gradient, (b) SGS, (c) convective term, (d) Poisson solver, and (e) total time loop. The numerical resolution is 128^3, run with 64 MPI processes, and a domain decomposition of 8×8

~~to increase with resolution increases)~~, the overall cost of the convective term will remain important regardless of the changes in numerical resolution. The goal of this work is to explore the possibility of using alternative dealiasing techniques to enhance the computational performance, while maintaining accurate turbulent flow statistics in simulations of ABL flows. It is important to note that the SGS model used here takes a relatively small fraction of the time integration. This fraction is likely to be larger if a more sophisticated model is used, for example the dynamic Smagorinsky model (Germano et al., 1991) or the Lagrangian scale dependant model (Bou-Zeid et al., 2005). In addition, it is important to note that the low computational cost of the Poisson solver is related to the the use of the pencil decomposition, which takes full advantage the pseudo-spectral approach. Specifically, the Z-pencil combines with the horizontal treatment of the derivatives to make the implementation of the solver very efficient.

3.4 Study cases

The goal of this study is to develop a cost benefit analysis for the different, already established, dealiasing methods from a computational cost stand point as well as in terms of accuracy in reproducing turbulent flow characteristics. For this reason, three different cases have been considered corresponding to the three dealiasing methods considered: (a) the 3/2-rule used as reference, (b) the Fourier truncation method (FT), and (c) the Fourier smoothing method (FS). All the simulations have been run with a numerical resolution of $N_x \times N_y \times N_z = 64^3$, 128^3, 192^3 and 256^3 with a domain size of $(L_x, L_y, L_z) = (2\pi, 2\pi, 1) \cdot z_i$, where z_i is the height of the boundary layer taken here with a value of $z_i = 1000$ m. A uniform surface roughness of value ~~$z_0/z_i = 10^{-5}$~~ $z_0/z_i = 10^{-4}$ is imposed, which is representative of sparse forest or farmland with many hedges ~~(Stull, 1988) (p.380)~~(Brutsaert, 1982; Stull, 1988). The simulations have been initialized with a vertical logarithmic profile with added random noise for the $\tilde{u}_1$ component. The two other velocity components $\tilde{u}_2$ and $\tilde{u}_3$ have been initialized with an averaged zero velocity profile with added noise to generate the initial turbulence. The integration time step is set to $\Delta t = 0.2$ s for ~~both~~ the 64^3~~, and~~ -, 128^3~~simulations and~~ -, and the 192^3-simulations and to $\Delta t = 0.1$ s for the 256^3~~simulation~~-simulation. These time steps ~~have been set to keep the equivalent CFL number bounded throughout the simulation~~ensure that stability requirements for the time-integration scheme are met. The Smagorinsky constant and the wall damping exponent are set to $C_S = 0.1$ and $n = 2$ (Mason, 1994; Porté-Agel et al., 2000; Sagaut, 2006).

For each dealiasing method, the simulations at 64^3, ~~and~~ 128^3, 192^3, and 256^2 were run until the flow reached statistic convergence of the friction velocity u_* and the mean kinetic energy. This warm-up time was fixed to $\sim 95T$ (where T is the flow-through time, defined as $T = U_\infty t / L_x$). At this point, running averages were computed to evaluate the different flow statistics presented in the following sections. ~~The simulations~~ To provide long enough averaging times, the 64^3- and 128^3-simulations were run for an additional $\sim 190T$~~, providing long enough averaging times. The~~. The 192^3- and 256^3~~simulation was run for $\sim 67T$ because of computational resource restrictions~~-simulations were run for an additional $\sim 100T$. In parallel, runs with higher horizontal resolution were used to evaluate the computational cost of the dealiasing methods with increasing numerical resolution (timing runs). These last simulations were only run for a few thousand iterations. Table 1 contains a summary of all the simulations preformed in this work.

Simulation type	Resolution $N_x \times N_y \times N_z$	Flow-through time T
Statistics runs	$64 \times 64 \times 64$	$\sim 285T$
	$128 \times 128 \times 128$	$\sim 285T$
	$192 \times 192 \times 192$	$\sim 200T$
	$256 \times 256 \times 256$	~~$\sim 67T$~~ $\sim 200T$
Timing runs	$128 \times 128 \times 128$	$\sim 2T$
	$256 \times 256 \times 128$	$\sim 2T$
	$512 \times 512 \times 128$	$\sim 2T$
	$1024 \times 1024 \times 128$	$\sim 2T$
	$2048 \times 2048 \times 128$	$\sim 2T$

Table 1. Simulations summary, each simulation was run with the three different dealiasing methods.

4 Results

4.1 Computational cost

~~Computational cost of the convective module as a function of the horizontal resolution. The timing of the module is presented on the left vertical axis and represented by left-pointing arrows. The number of operation is shown on the right vertical axis and represented by right-pointing arrows. The three different dealiasing methods are plotted as 3/2-rule in dot-dashed line, FT method in dotted line and FS method in dashed line. The numerical resolutions are $n_x \times n_y \times 128$, run with 64 MPI processes, and a domain decomposition of 8×8~~

~~To evaluate the effectiveness of the FT and FS methods, the~~ The computational cost of ~~these two methods has been computed and compared to the computational cost of the original~~ evaluating the convective term, dealiased via the the 3/~~2-rule method. Figure 5 presents the corresponding cost of the FTand FS methods for the convective term as it is the only one affected by the dealiasing method~~2 rule, the FT, and the FS are inter-compared in Figure 5. The horizontal resolution has been increased from 128×128 to 2048×2048 ~~to evaluate the performance across different grid resolutions~~collocation nodes to highlight how the different methods scale. Only the horizontal resolution is changed given that the vertical direction is treated in physical space with ~~finite difference methods and does not~~ second-order accurate centered finite difference method. Note that such a method does not typically require any dealiasing treatment, because the truncation error ~~associated with the second order centered finite difference method decreases the~~ tends to decrease the aliasing errors (Kravchenko et al., 1996; Canuto et al., 2006). In figure 5, the ordinate axis are divided by $n_x \cdot n_y$ to show the effect of the increase in resolution on the computational cost. The number of MPI processes and the domain decomposition have been kept identical to avoid introducing effects from the parallelization scaling into the results. Hence, only the effect of the resolution change on the computation time of the dealiasing methods is presented here. Results confirm that the computational cost of the convective term is ~~significantly~~ notably smaller when using the FT and FS dealiasing methods, with gains ~~between 20% and 30%, depending on the numerical resolution.~~ of 30% at $n_x \times n_y = 128 \times 128$ and 23% at $n_x \times n_y = 2048 \times 2048$. The results follow the ~~predicted computational cost predicted~~ computational cost calculated by the number of operations presented in section 2 ~~. The small~~ which predicted a gain of up to 35% for runs with 4096^3 grid nodes. The deviation in the computational cost present in figure 5 is the result of the varying load of the computer cluster since all simulations were run using the same number of nodes to avoid having to add the code's scaling properties to the analysis. From the results it is also important to note that there is no significant difference in the computational cost between the FT and FS methods, given that both use the same grid size and hence the corresponding numerical complexity of both methods is similar. ~~Therefore, as initially expected, results show that the less used FT and FS dealiasing methods have a clear impact on the performance of the code, yielding a net gain between 20% and 30% over the traditional 3/2-rule.~~ It is also ~~important to note~~ worth mentioning that these methods are ~~quite simple to implement given that~~ simpler to implement and require less rapid-access memory when compared to the 3/2 rule, as there is no need ~~for artificially extending~~ to extend neither the numerical grid ~~.~~ nor the wavenumber range.

In the following subsections, we compare the ~~effects~~ impact of the different dealiasing schemes on ~~the turbulent flow characteristics and quantify the differences. The goal is to clarify the extend of the perturbations introduced on the flow field if the more economical and less cumbersome FT and FS dealiasing techniques were to be implemented~~flow statistics. Profiles from runs using the 3/2-rule for dealiasing will be taken as reference and comments will focus on departures from such "exact" profiles when the FT or FS treatments are considered.

4.2 Flow statistics

Traditional flow metrics are investigated next and compared between the different dealiasing schemes. ~~Apart from figure 6 which shows the 256^3-case, results~~ Results for the 128^3 ~~-case~~ , 192^3, and 256^3-cases are presented in this section. The ~~findings of the 64^3-case are not shown because they are very similar to the 128^3-case. The~~ results are normalized using the traditional

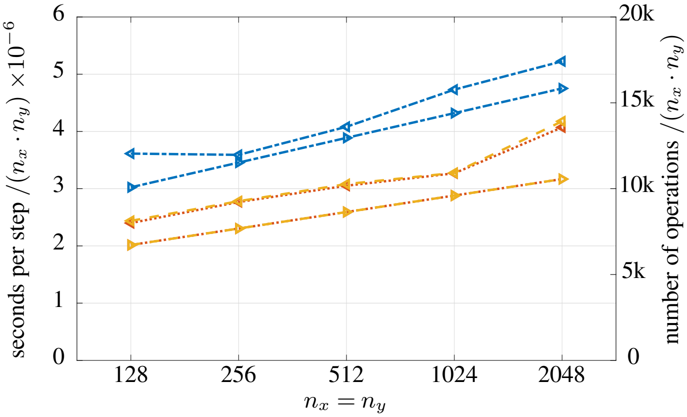

Figure 5. Computational cost of the convective module as a function of the horizontal resolution. The timing of the module is presented on the left vertical axis and represented by left-pointing arrows. The number of operation is shown on the right vertical axis and represented by right-pointing arrows. The three different dealiasing methods are plotted as 3/2-rule in blue dot-dashed line, FT method in orange dotted line and FS method in yellow dashed line. The numerical resolutions are $n_x \times n_y \times 128$, run with 64 MPI processes, and a domain decomposition of 8×8

scaling variables: the friction velocity (u_*) and the boundary layer height (z_i). As a starting point, figure 6 shows an instantaneous snapshot (pseudo-color plots) of the ~~strea-mwise~~ streamwise velocity perturbation for the three dealiasing methods. An additional case without dealiasing in the convective term was run and resulted in a complete laminarization of the turbulent flow (not showed here)~~. In the latter case, the flow completely laminarized throughout, destroying the turbulence, highlighting the extreme~~ , highlighting the importance of the dealiasing operation (Kravchenko and Moin, 1997). On the contrary, when dealiasing schemes are applied, the instantaneous flow field appears ~~quite~~ qualitatively similar among the different cases. Irrespective of the dealiasing method that is used, ~~stream-wise elongated uniform~~ streamwise elongated high- and low-momentum bulges flank each other, as apparent in figure 6. This is a common phenomena in pressure-driven boundary-layer flows (Munters et al., 2016). Qualitatively, small differences can be appreciated on the structure and distribution of the smaller-scale turbulence within the flow ~~. This is expected given the explicit filtering used in the latter dealiasing schemes (the FT and FS)~~only in the FT method. For example, the flow in subplot *b* is showing the effect of the cut-off filter, ~~as small circular structures can be observed. Thus, the FT methods is changing the nature of the small scales in the turbulent flow field. Alternatively, the stream-wise velocity obtained with the FS method does not seem to be as affected by these artifacts. Note however that these differences are in the instantaneous field, whose intrinsic nature is unsteady and chaotic. A more quantitative analysis follows.~~ which high frequency perturbations throughout the considered pseudocolor plot. These spurious oscillations have an impact on the flow statistics, as will be shown in the following.

~~A step in that direction is made through the analysis of the averaged velocity profiles and the velocity gradients, shown in figure 7. Profiles show a good~~ The horizontally- and temporally-averaged velocity profiles are characterized by an approximately logarithmic behavior within the surface-layer (~~$z \sim 0.1 z_i$) for all cases, matching the imposed boundary conditions,and represented~~

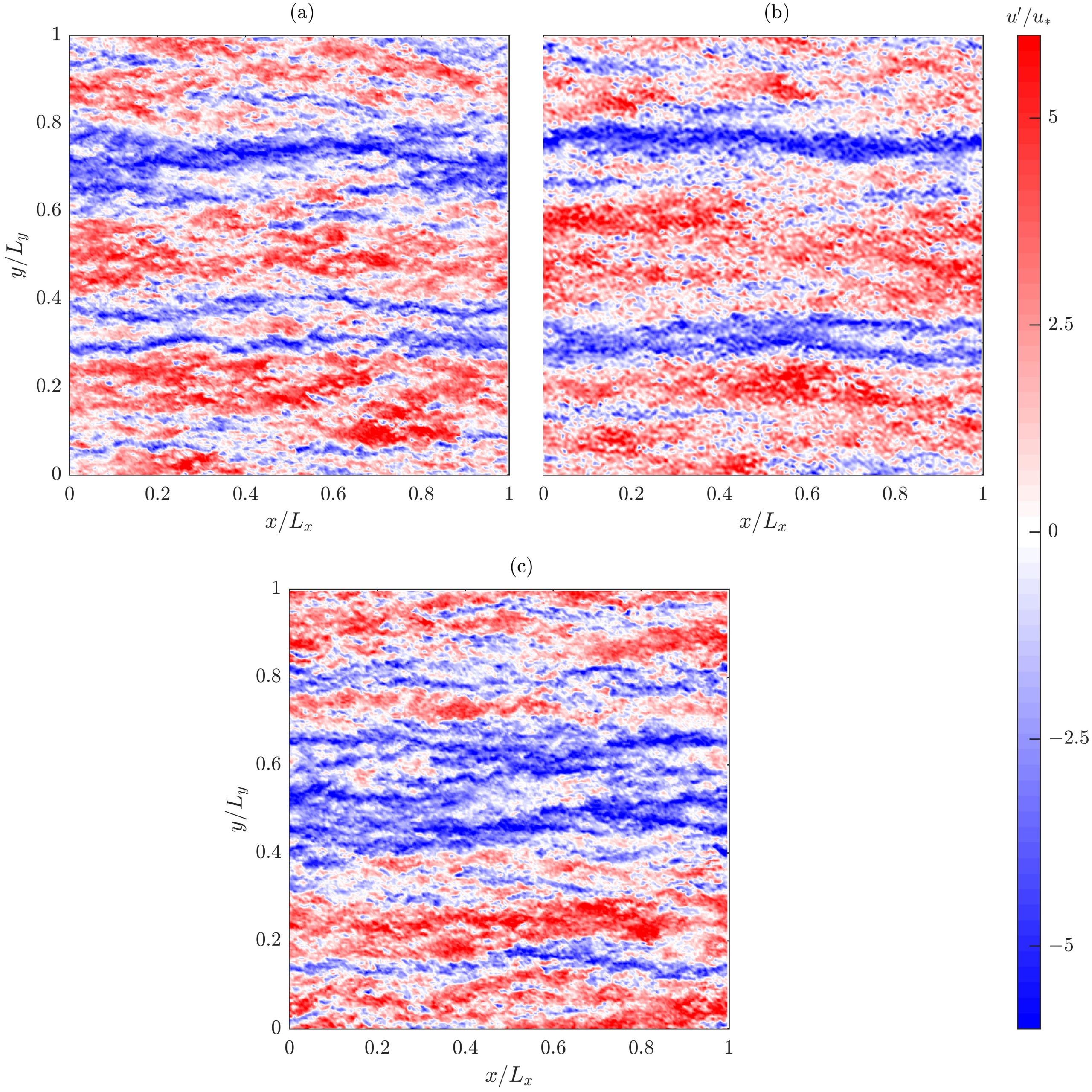

Figure 6. Instantaneous streamwise velocity perturbation $u'(x,y,z,t) = u(x,y,z,t) - \bar{u}(x,y,z)$ at $z/z_i = 0.027$ for the three different dealiasing methods: (a) 3/2-rule, (b) FT method, and (c) FS method. The numerical resolutions is 256^3.

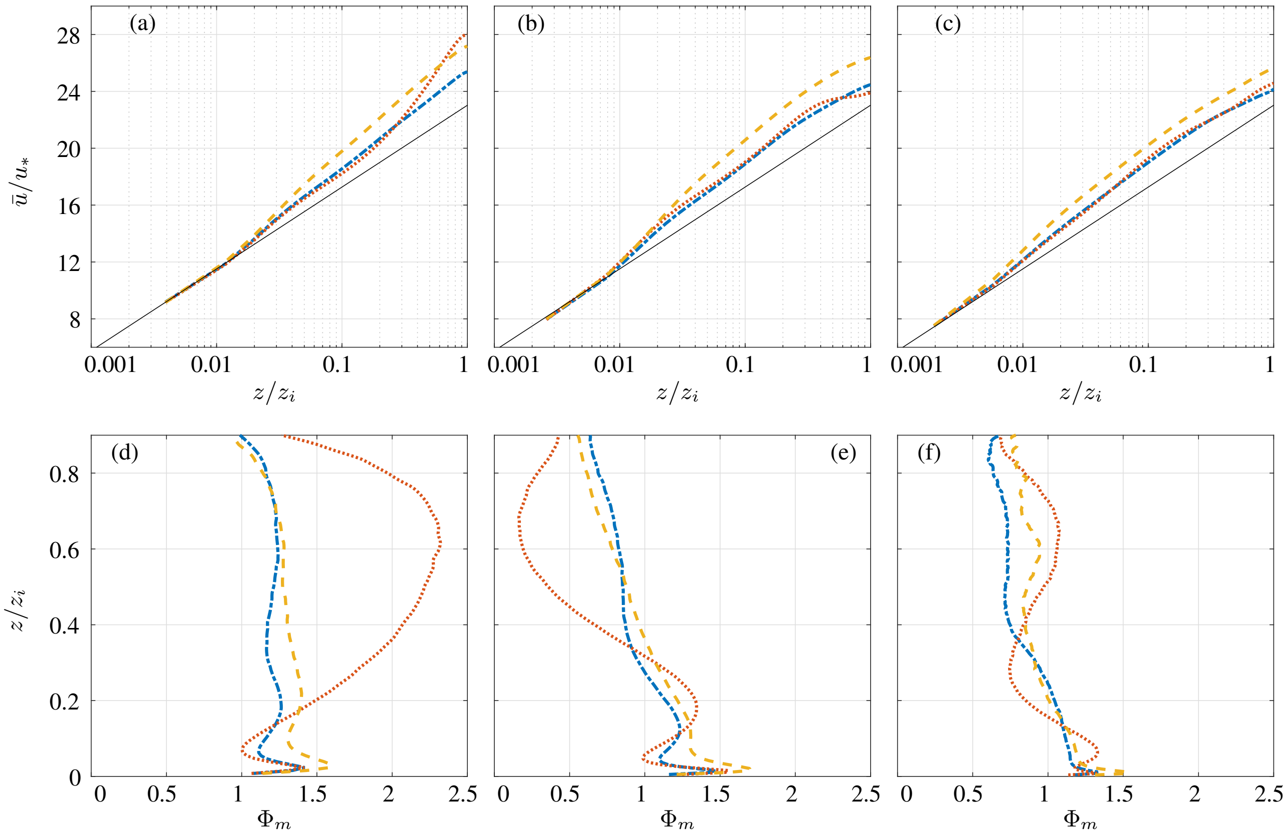

Figure 7. ~~Plots~~ Top panels represent the plots of the non-dimensional mean streamwise velocity profile for (a) the 128^3-case, (b) the 192^3-case, and (c) the 256^3-case. Bottom panels represent the mean ~~stream-wise~~ streamwise velocity gradient for (~~b~~d) ~~for~~ the 128^3-case, (e) the 192^3-case, and (f) the 256^3-case. The lines represent the three different dealiasing methods: 3/2-rule in blue dot-dashed line, FT method red in dotted line and FS method in yellow dashed line. The solid line ~~in (a)~~ represents the ideal log-law profile.

~~with the solid line. Specifically, the FT method exhibits a good overlap up to $z \sim 0.4z_i$~~ $z \approx 0.15z_i$, as apparent from Fig. 7, where results are illustrated for the three resolutions: 128^3,192^3, and 256^3). For the 128^3 case, the observed departure from the logarithmic profile for the 3/2-rule case is in excellent agreement with results from previous literature for this particular SGS model (Porté-Agel et al., 2000; Bou-Zeid et al., 2005). When using the FT method the agreement of the averaged velocity profile with the ~~velocity profile obtained using the~~ corresponding 3/2-rule ~~. A maximum momentum departure of $\sim 14\%$ is measured at the top of the domain. On the other hand,~~ profiles improves with increasing resolution. While in the 128^3 case a good estimation of the logarithmic flow is obtained at the surface layer, there is a large acceleration of the flow further above. This overshoot does not occur for the higher resolution runs. When using the FS method~~presents a weaker differentiated behavior of only $\sim 7\%$ from $z \sim 0.05z_i$ up to the top of the domain. These~~ , the mean velocity magnitude is consistently over-predicted throughout the domain, and the situation does not improve with increasing resolution (the overshoot is up to 7.5% for the 128^3, 8.5% for the 192^3 and 7% for the 256^3 run). Further comparing the results obtained by the FS and FT method with those obtained with the 3/2-rule, it is clear that while the FS method presents a generalized overestimation of the velocity with a an overall good logarithmic trend, the FT method presents a better adjustment in the surface layer with larger departures from the logarithmic regime on the upper domain region that get reduced with increasing numerical resolution. The mean ~~stream-wise velocity above the surface layer by the FS method leads to an overall increase of $\sim 15\%$ on the mean~~ kinetic energy ~~(MKE)~~ of the system ~~. Otherwise, when using~~ is overestimated by $\approx +2\%$ and $\approx +12\%$ by the FT and FS methods, when compared to that of runs using the 3/2-rule in the ~~FT method the overshoot in mean velocity seems to be reduced to the top of the numerical domain, hence leading to a weaker overall increase in MKE of $\sim 11\%$. This increase in MKE~~ 256^3 case. Overall, the mean kinetic energy is larger for the FT and FS cases, when compared to the 3/2-rule case, even at the highest of the considered resolutions ($\approx +2\%$ and $\approx +12\%$ by the FT and FS methods for the 256^3 case). Such behavior can be related to the low-pass filtering operation that is performed in the near-wall regions~~by the FT and FS methods, which modify the balance between turbulent and laminar stresses at such location, in favor of the laminar component, thus~~ , which tends to reduce resolved turbulent stresses in the near-wall region, resulting in a higher mass flux for the considered flow system. This is more apparent for the low resolution cases. ~~Note that the low-pass filtering operation performed by the FT and FS methods has similar effects to increasing the LES eddy-diffusivity.~~

~~Complementary to the mean velocity profiles, figure 7 (b) presents the normalized velocity gradient, $\Phi_m = \kappa \frac{z}{u_*}\partial_z \langle U \rangle_{xy}(z)$. In all cases, it presents~~ Mean velocity gradient profiles ($\Phi_m = \kappa \frac{z}{u_*}\partial_z \langle U \rangle_{xy}(z)$) are also featured in Figure 7 (d, e, f). Profiles at each of the considered resolutions present a large overshoot near the surface, which is a well known ~~LES problem of wall bounded~~ problem in LES of wall-bounded flows and has been extensively discussed in the literature (Bou-Zeid et al., 2005; Brasseur and Wei, 2010; Lu and Porté-Agel, 2013). ~~The high gradient near the wall suggests that the resolved kinetic energy is over dissipated by the Smagorinsky model close to solid boundaries, even with the Mason-Thompson damping wall function. Therefore, the overall turbulent stresses are too low there, resulting in an overestimated mean velocity in the bulk of the flow. Again, such over-dissipative behavior is further aggravated when applying the FS or the FT methods. From the vertical gradient profiles~~ In comparing the results between the FS and FT method with the 3/2-rule, it can be observed that ~~the three methods produce similar results~~ there are stronger gradients in the mean velocity profile within the surface layer ~~. Above that, the FS follows very well the profile provided by the 3/2-rule. Contrary, the truncation methodover-estimates the velocity gradient starting from $z = 0.2z_i$ up to the top of the domain. This is an important result because it shows that despite the over-dissipative behavior of the FS method, its vertical distribution remains similar to that obtained with the 3/2-rule. Contrary, with~~ when using the FS method. This leads to the observed shift in the mean velocity profile. Conversely, when using the FT method~~there exists both, a stronger over-dissipation of turbulent motions in the near wall regions, inducing a higher mass flux, and a differentiated momentum distribution throughout the domain. This results from the fact that when using the FT method a broader range of energetic near-wall coherent structures are removed, hence having a larger effect on the overall vertical distribution of momentum~~, departures are of oscillatory nature, leading to less pronounced variations in the mean velocity profile when compared to the reference ones (the 3/2-rule cases). This behavior is consistently found across the considered resolutions, but the situation ameliorates as resolution is increased (*i.e.* weaker departures).

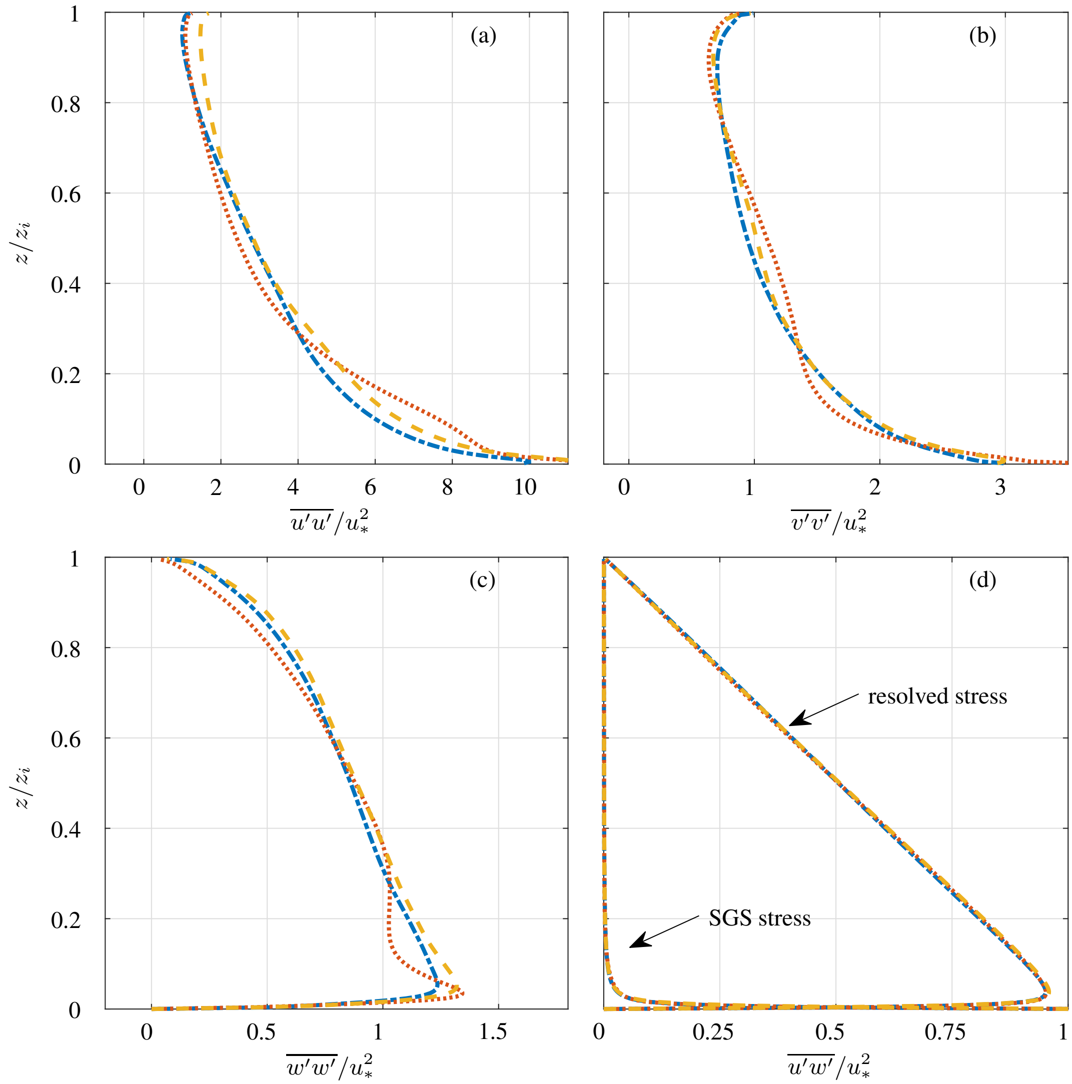

Figure 8. Profiles of the non-dimensional variances (a/b/c) and shear stress (d) for the three different dealiasing methods: 3/2-rule in blue dot-dashed line, FT method in red dotted line and FS method in yellow dashed line.

~~Next we investigate the effect of the simpler and computationally faster dealiasing-schemes on the second order moments. The~~ Figure 8 features the vertical structure of ~~variances $\overline{u'u'}$,$\overline{v'v'}$,$\overline{w'w'}$ and of the turbulent stress $\overline{u'w'}$ are featured in figure 8, where $\overline{(\cdot)}$ denotes the space + time averaging operator, and $(\cdot)'$ denotes a fluctuation from the corresponding average value~~second order statistics predicted via the FS and the FT methods, including a comparison with the corresponding predictions from the 3/2 rule, 256^3 study case. Note that when averaging in space and (subsequently) in time, ~~dispersive terms are embedded in the variance and covariance terms (Raupach et al., 1991; Finnigan, 2000). The~~ the resulting profiles are comparable to those found in previously published LES studies ~~(Porté-Agel et al., 2000; Bou-Zeid et al., 2005).~~

~~Interestingly, results of the vertical flux (or stress , resolved and SGS) of stream-wise momentum (figure 8(d)) illustrate a good agreement between the different scenarios. Contrary, larger differences appear in the diagonal components of the turbulent stress tensor. For example, the stream-wise variance is underestimated by the FT method in the~~ (see *e.g.* Porté-Agel et al., 2000; Bou-Zeid et The fact that the shear stress profiles are similar among the different dealiasing cases is also indicative that the SGS fraction is not strongly affected by the choice of dealiasing method, which is also partly due to the simplicity of the Static Smagorinsky model that is being used. The potential effect that the different dealiasing schemes could have in more advanced subgrid models is discussed later on. Specifically, the error in the Reynolds shear stress (*e.g.* not including the SGS contribution) in the surface-layer ~~and up to almost $0.5z_i$. This underestimation is probably the one causing the apparent differences earlier observed qualitatively in the instantaneous velocity fields from Figure 6. On the other hand,~~ decreases with increasing resolution for the FS method (from 1.7% to 1.1% for the 128^3 and 256^3 respectively) as indicated in Table 2, and fluctuates also around very small values for FT method. When considering the diagonal stress tensor components across simulations, it is noteworthy that all such quantities are overpredicted when using the FT and the FS methods in the near surface region ($z \lesssim 0.15$). Further above, the ~~cross-stream and vertical variances are both slightly overestimated by the FS and FT methods. In all cases, the overestimation ceases near $0.5z_i$, and while for the cross-stream variances initiates at the surface, the overestimation on the vertical variances initiates towards the top of the surface-layer. It is important to note again, that~~ FS method tends to consistently overpredict, whereas the ~~FS method, while slightly diverging in absolute values (maximum divergence of 15%), it presents a very similar vertical distribution of the variances compared to the reference values obtained with the 3/2 rule. Contrary, the~~ FT method ~~diverges both, in absolute magnitude (maximum divergence of 35%) and vertical distribution, specially in the vertical variance. Once again, this is the result of the different filtering operations applied to the small turbulence scales during the integration of the NS equations~~present an oscillatory nature. As can be observed in Table 2, the mean error deviations decrease with increasing resolution, for all cases, except for the streamwise variance where there is no clear trend.

case	method	$err(\overline{u'u'})$	$err(\overline{v'v'})$	$err(\overline{w'w'})$	$err(\overline{u'w'})$
128^3	FT	21.5%	20.8%	19.8%	0.3%
128^3	FS	5.0%	16.7%	9.5%	1.7%
192^3	FT	6.8%	17.3%	21.3%	2.4%
192^3	FS	13.4%	18.1%	12.0%	1.5%
256^3	FT	20.8%	7.8%	8.5%	0.3%
256^3	FS	10.5%	3.4%	5.5%	1.1%

Table 2. Mean error on the variance profiles between the FT/FS methods and the 3/2-rule over the lower 15% of the domain. For example the error of the streamwise variance is computed as $err(\overline{u'u'}) = \frac{1}{n}\sum\left|1 - \frac{\overline{u'u'}^{FT/FS}}{\overline{u'u'}^{3/2}}\right|$ for $0 < z < 0.15 \cdot z_i$.

To complement the analysis of the effect of the different dealiasing methods on the physical structure of the flow, the corresponding power spectra is investigated. According to Kolmogorov's energy cascade theory, the inertial sub-range of the power ~~spectra~~ spectrum should be characterized by a power law of $-5/3$ slope (Kolmogorov, 1968). In this range the effects of viscosity, boundary conditions, and large scale structures are not important. Also, in wall-bounded flows ~~with neutral buoyancy~~ without buoyancy effects, a production range should also be present, following a power-law scaling of -1 (Gioia et al., 2010; Katul et al., 2012; Calaf et al., 2013). Figure 9 shows the energy spectra of the ~~stream-wise~~ streamwise velocity obtained using the different dealiasing methods. The spectrum obtained using the 3/2-rule matches well the traditional turbulent spectra presented in the literature (Cerutti, 2000; Bou-Zeid et al., 2005) and it is used to assess the effects introduced by the FT and FS dealiasing methods. From this spectral analysis, it can be observed that ~~low wave-number modes in the spectra are very similar between the 3 methods and only the~~ the high wave-number ranges are modified ~~. The~~ by both methods. The FT method sharply cuts the spectra at the scale of $3/2 \cdot \Delta$ close to the LES filter scale Δ. On the other hand, the FS method smoothly attenuates the effects of the aliasing errors at the high-end of the spectra. The dealiasing methods have been designed for such behavior, since only the higher frequencies are filtered. From the FT method flow field spectra it is clearly visible the effect of the cut-off applied within the dealiasing scheme. It is apparent that the capacity of the LES solver to reproduce the fine scale turbulence structure of the flow is strongly jeopardized when using the FT method and limited at the scale of $3/2 \cdot \Delta$ close to the LES filter scale Δ. Essentially, this method artificially over-dissipates the turbulent kinetic energy and yields to an overestimation of the mean kinetic energy. In contrast, ~~and as one would expect,~~ the energy spectrum obtained using the FS method does not produce such a large energy cut-off~~because the high wave-numbers are only smoothed to attenuate the effects of the aliasing errors~~. Therefore, a larger range of the spectrum is resolved and less turbulent kinetic energy is dissipated by aliasing errors. ~~In conclusion, the FS method produces an energy spectra that reproduces most of the observed features of the fully dealiased spectra (3/2-rule)at a reduced computational cost .~~

Although the effect of the FT and FS methods on the small scale can be clearly observed in figure 9, their effect on the large scales also needs to be quantified. To compute a direct comparison scale by scale, the following ratio was used (equation 16) for the 128^3, 192^3, and 256^3-simulations,

$$\rho^{XX}(k) = \frac{E^{XX}_{u,k} - E^{3/2}_{u,k}}{E^{3/2}_{u,k}} \tag{16}$$

where $E_{u,k}$ denotes the power spectral density of the u velocity component at wavenumber k, XX stands for the dealiasing method FT or FS. If $\rho(k) < 0$ the energy density at that given wavenumber (k) is less than the corresponding one for the run using the $3/2$ rule, viceversa if $\rho(k) > 0$. Figure 10 presents the ratio $\rho(k)$ for both methods.

When using the FT method, energy at the low wavenumbers is underpredicted, whereas energy at the large wavenumbers is overpredicted. Departures are in general larger with decreasing resolution, with an excess of up to 100% for the 128^3-simulations in the wavenumber range close to the cutoff wavenumber. On the contrary, when using the FS method, the energy from the filtered (dealiased) small-scales is redistributed quasi-uniformly throughout the spectra with an averaged overall variation of less than 13%.

5 Discussion

~~Normalized stream-wise spectra of the stream-wise velocity as a function of $k_x z$ for the three different dealiasing methods: 3/2-rule (a), FT method (b), FS method (c) at height $z/z_i = 0.0117$, 0.0273, 0.0586, 0.0898, 0.1523, 0.2148, 0.3086, 0.4336, 0.5586, and 0.6211.~~

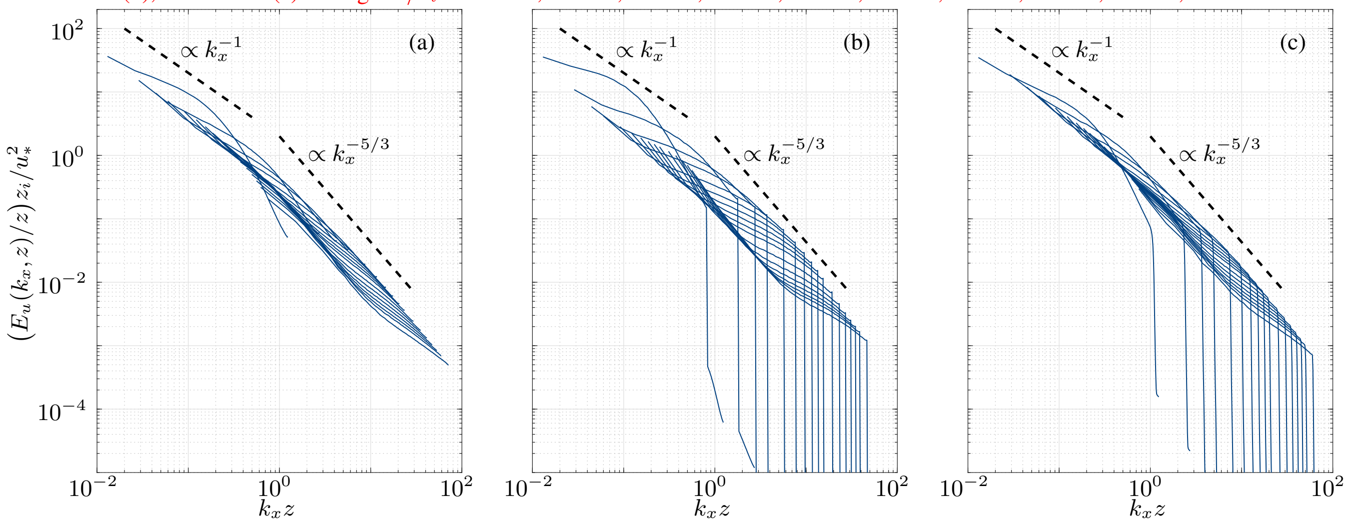

Figure 9. Normalized streamwise spectra of the streamwise velocity as a function of $k_x z$ for the 192^3-simulations. The three different dealiasing methods are 3/2-rule (a), FT method (b), FS method (c) at heights $z/z_i = 0.0117$, 0.0273, 0.0586, 0.0898, 0.1523, 0.2148, 0.3086, 0.4336, 0.5586, and 0.6211.

In the development of this manuscript, focus has been directed to the study of the advantages and disadvantages of different dealiasing methods. In this regard, throughout the analysis we have tried to keep the structure of the LES configuration as simple and canonical as possible, to remove the effect of other add-on complexities. Additional complications might arise when considering additional physics; here we discuss the potential effect that these different dealiasing methods could have on them. One of such elements of added complexity is for example the use of more sophisticated subgrid scale models based on dynamic approaches to determine the values of the Smagorinsky constant (Germano et al., 1991; Bou-Zeid et al., 2005). In most of these advanced subgrid models, information from the small-scale turbulent eddies is used to determine the evolution of the subgrid constant. However, in both the FT and FS method, the small turbulent scales are severely affected and hence use of dynamic subgrid models could be severely hampered unless these are accordingly modified and adjusted, maybe via filtering at larger scales than the usual grid scale. Another element of added complexity consists in using more realistic atmospheric forcing, considering for example the effect of the Coriolis force with flow rotation as a function of height and velocity magnitude. In this case, we hypothesize that the FT method could lead to stronger influences on the resultant flow field as this dealiasing technique not-only affects the distribution of energy in the small turbulent scales, but also in the large scales (as apparent from Fig. 10), being these later ones potentially more affected by the Coriolis force. This represents a strong non-linear effect, that is hard to quantify and hence further testing, including realistic forcing with a geostrophic wind and Coriolis force would be required to better quantify these effects. Also often in LES studies of atmospheric flows one is interested in including an accurate representation of scalar transport (passive/active). In this case the differential equations don't include a pressure term

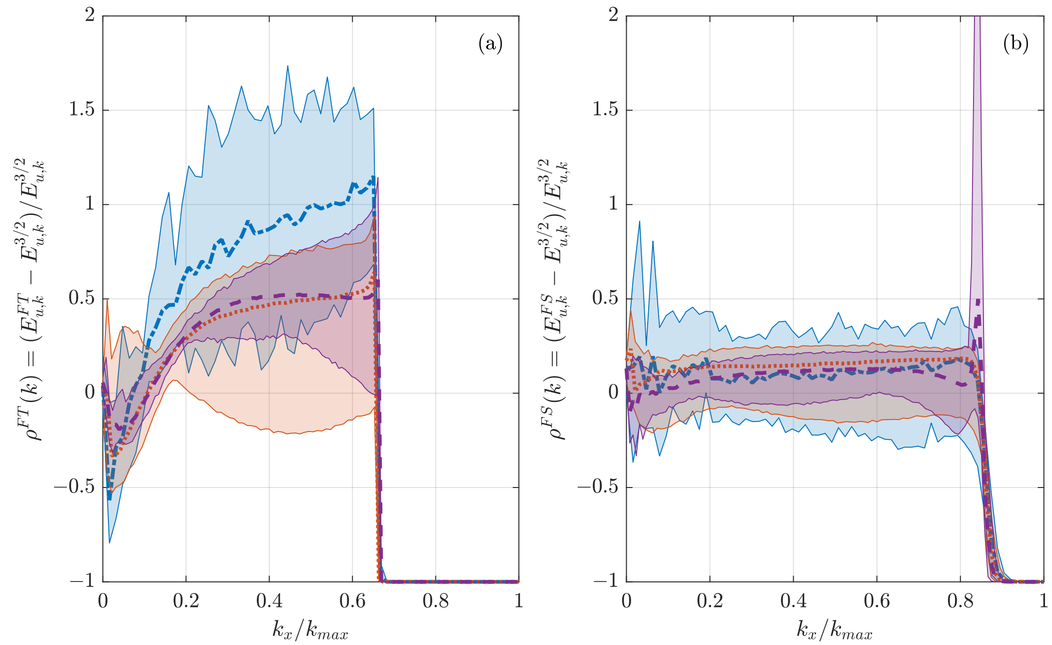

Figure 10. Effect of the FT (a), and the FS (b) methods of the streamwise spectra of the streamwise velocity compare to the 3/2-rule. The solid line represent the average value and the shaded area represent the extreme values. The resolutions are: 128^3 in blue dot-dashed line, 192^3 in red dotted line, and 256^3 in purple dashed line.

and hence most of the computational cost is linked to the evaluation of the convective term. As a result, the benefit of using alternative, cheaper dealiasing techniques (FT or FS) will be even more advantageous, yet the total gain is not trivial to evaluate *a priori*, and the effect on the scalar fields should also be further evaluated.

In general, we believe that it is not fair to advocate for one or other dealiasing method based on the results of this analysis. Note that the goal of this work is to provide an objective analysis of the advantages and limitations that the different methods provide, letting the readers the ultimate responsibility to choose the option that will adjust better to their application. For example, while having exact dealiasing (3/2-rule) might be better in studies focusing on turbulence and dispersion, one might be well-off using a simpler and faster dealiasing scheme to run the traditionally expensive warm-up runs, or to evaluate surface drag in flow over urban and vegetation canopies, where most of the surface force is due to pressure differences (Patton et al., 2016).

6 Conclusions

The Fourier-based pseudo-spectral collocation method (Orszag, 1970; Orszag and Pao, 1975; Canuto et al., 2006) remains the preferred “work-horse" in simulations of wall-bounded flows over horizontally periodic regular domains, which is often used in conjunction with a centered finite-difference or Chebychev polynomial expansions in the vertical direction (Shah and Bou-Zeid, 2014; Moeng and Sullivan, 2015). This approach is often used because of the high-order accuracy and the intrinsic efficiency of the fast-Fourier-transform algorithm (Cooley and Tukey, 1965; Frigo and Johnson, 2005). In this technique, ~~the leading-order error term is the~~ aliasing that arises when evaluating the quadratic non-linear term in the NS equations ~~. Aliasing errors~~ can severely deteriorate the quality of the solution ~~, even leading to laminarization of turbulent flows,~~ and hence need to be treated adequately. In this work a performance/cost analysis has been developed for three well-accepted dealiasing techniques (3/2-rule, FT and FS) to evaluate the corresponding advantages and limitations. ~~Note that~~ The 3/2-rule requires a computationally expensive padding and truncation operation, while the FT ~~method applies a cut-off filter at the scale of $3/2 \cdot \Delta$ (close to the LES filter scale Δ), the FS method uses a smooth filter to attenuate the effects of the aliasing errors, hence progressively attenuating the effect of the smaller turbulent scales.~~ and FS methods provide an approximate dealiasing by low-pass filtering the signal over the available wavenumbers, which comes at a reduced cost.

~~A very important result is the fact that computational cost is reduced by 20% to 30% when using the FS or FT methods, respectively, depending on~~ The presented results show compelling evidence of the benefits of these methods as well as some of their drawbacks. The advantage of using the FT or the FS approximate dealiasing methods is their reduced computational cost ($\sim$15% for the 128^3 case, $\sim$25% for the 256^3 case), with an increased gain as the numerical resolution is increased. Regarding the flow statistics, results illustrate that both, the FT and the FS methods, yield less accurate results when compared to those obtained with the traditional 3/2-rule, as one could expect. ~~In this regard, results are aligned with the theoretical predictions despite of parallelization and domain decomposition, indirectly illustrating the robustness of the LES platform here used.~~

~~To evaluate the influence of these two dealiasing schemes beyond the computational cost, traditional flow statistics have been evaluated. The~~ Specifically, results illustrate that both the FT and FS methods over-dissipate the ~~FT method over-dissipates the~~ turbulent motions in the near wall ~~regions, inducing a~~ region, yielding an overall higher mass flux ~~, and a different velocity distribution throughout the domain~~ when compared to the reference one (3/2-rule). Regarding the variances, results illustrate modest errors in the surface-layer, with local departures in general below 10% of the reference value across the considered resolutions. The observed departures in terms of mass flux and velocity variances tend to reduce with increasing resolution. Analysis of the streamwise velocity spectra has also shown that the FT method redistributes unevenly the energy across the available wavenumbers, leading to an over-estimation of the energy of some scales by up to 100%. Contrary, ~~when comparing the FS method against full dealiasing, similar vertical distributions in momentum and second-order statistics are obtained, despite the additional dissipation that such approximate methods introduce (via damping of small scale motions). These~~ the FS methods redistributes the energy evenly, yielding a modest +13% energy magnitude throughout the available wavenumbers. Compared to the 3/2-rule, these differences in flow statistics ~~between the FT and FS methods~~ are the result of the sharp low-pass filter applied in the FT method ~~compared to the smoothing function used in the FS method. Although the simulations presented in this paper do not account for the Coriolis Effect (flow rotation) results are very important for the ABL-modeling community. The effects of the dealiasing schemes affect more the small scale turbulence, and are mostly encountered in the surface layer, where rotational effects are minimal.~~

~~The results presented here show compelling evidence of the benefits of the FS method, providing important computational gains while producing similar instantaneous turbulence behavior (spectral analysis) and converged statistics to the commonly accepted 3/2-rule (full dealiasing)~~and the smooth filter that characterizes the FS method.

Code availability. The sources of the LES code developed at the University of Utah are accessible in pre-release at https://doi.org/10.5281/zenodo.1048338 (Margairaz et al., 2017).

Data availability. Due to the large amount of data generated during this study, no lasting structure can be permanently supported where to openly access the data. However, access can be provided using the Temporary Guest Transfer Service of the Center of High Performance Computing of the University of Utah. To get access to the data, Marc Calaf (marc.calaf@utah.edu) will provide temporary login information for the sftp server.

Competing interests. The authors declare no competing interests

Acknowledgements. F.M. and M.C. acknowledges the Mechanical Engineering Department at University of Utah for start-up funds. M.G.G and M.B.P. acknowledge the Swiss National Science Foundation (SNSF-200021- 134892), and the Competence Center for Environmental Sustainability (CCES-SwissEx) of the ETH domain. The authors would also like to recognize the computational support provided by the Center for High Performance Computing (CHPC) at University of Utah as well as the Extreme Science and Engineering Discovery Environment (XSEDE) platform (project TG-ATM170018).

References

Abkar, M. and Porté-Agel, F.: Mean and turbulent kinetic energy budgets inside and above very large wind farms under conventionally-neutral condition, Renewable Energy, 70, 142–152, https://doi.org/10.1016/j.renene.2014.03.050, 2014.

Albertson, J. D.: Large Eddy Simulation of Land-Atmosphere Interaction, Ph.D. thesis, University of California at Davis, Hydrologic Science, an optional note, 1996.

Albertson, J. D. and Parlange, M. B.: Natural integration of scalar fluxes from complex terrain, Advances in Water Resources, 23, 239–252, https://doi.org/10.1016/S0309-1708(99)00011-1, 1999.

Albertson, J. D., Parlange, M. B., Katul, G. G., Chu, C.-R., Stricker, H., and Tyler, S.: Sensible Heat Flux From Arid Regions: A Simple Flux-Variance Method, https://doi.org/10.1029/94WR02978, 1995.

Allaerts, D. and Meyers, J.: Boundary-layer development and gravity waves in conventionally neutral wind farms, Journal of Fluid Mechanics, 814, 95–130, https://doi.org/10.1017/jfm.2017.11, 2017.

Anderson, W., Passalacqua, P., Porté-Agel, F., and Meneveau, C.: Large-Eddy Simulation of Atmospheric Boundary-Layer Flow Over Fluvial-Like Landscapes Using a Dynamic Roughness Model, Boundary-Layer Meteorology, 144, 263–286, https://doi.org/10.1007/s10546-012-9722-9, 2012.

Bernaschi, M., Fatica, M., Melchionna, S., Succi, S., and Kaxiras, E.: A flexible high-performance Lattice Boltzmann GPU code for the simulations of fluid flows in complex geometries, Concurrency and Computation: Practice and Experience, 22, 1–14, https://doi.org/10.1002/cpe.1466, 2010.

Bou-Zeid, E., Meneveau, C., and Parlange, M. B.: Large-eddy simulation of neutral atmospheric boundary layer flow over heterogeneous surfaces: Blending height and effective surface roughness, Water Resources Research, 40, n/a–n/a, https://doi.org/10.1029/2003WR002475, 2004.

Bou-Zeid, E., Meneveau, C., and Parlange, M. B.: A scale-dependent Lagrangian dynamic model for large eddy simulation of complex turbulent flows, Physics of Fluids, 17, 025 105, https://doi.org/10.1063/1.1839152, 2005.

Bou-Zeid, E.: Challenging the large eddy simulation technique with advanced a posteriori tests, Journal of Fluid Mechanics, 764, 1–4, https://doi.org/10.1017/jfm.2014.616, 2014.

Bowman, J. C. and Roberts, M.: Efficient Dealiased Convolutions without Padding, SIAM Journal on Scientific Computing, 33, 386–406, https://doi.org/10.1137/100787933, 2011.

Brasseur, J. G. and Wei, T.: Designing large-eddy simulation of the turbulent boundary layer to capture law-of-the-wall scaling, Physics of Fluids, 22, 1–21, https://doi.org/10.1063/1.3319073, 2010.

Brutsaert, W.: Evaporation into the Atmosphere, Springer Netherlands, Dordrecht, https://doi.org/10.1007/978-94-017-1497-6, 1982.

Burkardt, J., Gunzburger, M., and Lee, H.-C.: POD and CVT-based reduced-order modeling of Navier–Stokes flows, Computer Methods in Applied Mechanics and Engineering, 196, 337–355, https://doi.org/10.1016/j.cma.2006.04.004, 2006.

Calaf, M., Meneveau, C., and Meyers, J.: Large eddy simulation study of fully developed wind-turbine array boundary layers, Physics of Fluids (1994-present), 22, 015 110, https://doi.org/10.1063/1.3291077, 2010.

Calaf, M., Meneveau, C., and Parlange, M. B.: Direct and Large-Eddy Simulation VIII, vol. 15 of *ERCOFTAC Series*, Springer Netherlands, Dordrecht, https://doi.org/10.1007/978-94-007-2482-2, 2011.

Calaf, M., Hultmark, M., Oldroyd, H. J., Simeonov, V., and Parlange, M. B.: Coherent structures and the k-1 spectral behaviour, Physics of Fluids, 25, https://doi.org/10.1063/1.4834436, 2013.

Canuto, C., Hussaini, M. Y., Quarteroni, A., and Zang, T. A.: Spectral Methods: Fundamentals in Single Domain, Springer-Verlag, Berlin, 2006.

Canuto, C., Hussaini, M. Y., Quarteroni, A., and Zang, T. A.: Spectral Methods: Evolution to Complex Geometries and Applications to Fluid Dynamics, Springer-Verlag, Berlin, 2007.

Cassiani, M., Katul, G. G., and Albertson, J. D.: The Effects of Canopy Leaf Area Index on Airflow Across Forest Edges: Large-eddy Simulation and Analytical Results, Boundary-Layer Meteorology, 126, 433–460, https://doi.org/10.1007/s10546-007-9242-1, 2008.

Cerutti, S.: Spectral and hyper eddy viscosity in high-Reynolds-number turbulence, Journal of Fluid Mechanics, 421, 307–338, 2000.

Chorin, A. J.: The numerical solution of the Navier-Stokes equations for an incompressible fluid, Bulletin of the American Mathematical Society, 73, 928–932, https://doi.org/10.1090/S0002-9904-1967-11853-6, 1967.

Chorin, A. J.: Numerical solution of the Navier-Stokes equations, Mathematics of Computation, 22, 745–762, https://doi.org/10.2307/2004575, 1968.

Cooley, J. W. and Tukey, J. W.: An algorithm for the machine calculation of complex Fourier series, Mathematics of Computation, 19, 297–297, https://doi.org/10.1090/S0025-5718-1965-0178586-1, 1965.

Finnigan, J.: Turbulence in Plant Canopies, Annual Review of Fluid Mechanics, 32, 519–571, https://doi.org/10.1146/annurev.fluid.32.1.519, 2000.

Frigo, M. and Johnson, S. G.: The design and implementation of FFTW3, Proceedings of the IEEE, 93, 216–231, https://doi.org/10.1109/JPROC.2004.840301, 2005.

Germano, M., Piomelli, U., Moin, P., and Cabot, W. H.: A dynamic subgrid-scale eddy viscosity model, Physics of Fluids A: Fluid Dynamics, 3, 1760–1765, https://doi.org/10.1063/1.857955, 1991.

Gioia, G., Guttenberg, N., Goldenfeld, N., and Chakraborty, P.: Spectral Theory of the Turbulent Mean-Velocity Profile, Physical Review Letters, 105, 184 501, https://doi.org/10.1103/PhysRevLett.105.184501, 2010.

Giometto, M. G., Christen, A., Meneveau, C., Fang, J., Krafczyk, M., and Parlange, M. B.: Spatial Characteristics of Roughness Sublayer Mean Flow and Turbulence Over a Realistic Urban Surface, Boundary-Layer Meteorology, https://doi.org/10.1007/s10546-016-0157-6, 2016.

Giometto, M. G., Christen, A., Egli, P., Schmid, M.F., Tooke, R.T., Coops, N.C., and Parlange, M. B.: Effects of trees on mean wind, turbulence and momentum exchange within and above a real urban environment, Advances in Water Resources, https://doi.org/10.1016/j.advwatres.2017.06.018, 2017.

Hamada, T., Narumi, T., Yokota, R., Yasuoka, K., Nitadori, K., and Taiji, M.: 42 TFlops hierarchical N -body simulations on GPUs with applications in both astrophysics and turbulence, in: Proceedings of the Conference on High Performance Computing Networking, Storage and Analysis - SC '09, c, p. 1, ACM Press, New York, New York, USA, https://doi.org/10.1145/1654059.1654123, 2009.

Horiuti, K.: Comparison of conservative and rotational forms in large eddy simulation of turbulent channel flow, Journal of Computational Physics, 71, 343–370, https://doi.org/10.1016/0021-9991(87)90035-0, 1987.

Hou, T. Y. and Li, R.: Computing nearly singular solutions using pseudo-spectral methods, Journal of Computational Physics, 226, 379–397, https://doi.org/10.1016/j.jcp.2007.04.014, 2007.

Hsu, M. C., Akkerman, I., and Bazilevs, Y.: High-performance computing of wind turbine aerodynamics using isogeometric analysis, Computers and Fluids, 49, 93–100, https://doi.org/10.1016/j.compfluid.2011.05.002, 2011.

Hughes, T. J. R., Cottrell, J. A., and Bazilevs, Y.: Isogeometric analysis: CAD, finite elements, NURBS, exact geometry and mesh refinement, Computer Methods in Applied Mechanics and Engineering, 194, 4135–4195, https://doi.org/10.1016/j.cma.2004.10.008, 2005.

Hultmark, M., Vallikivi, M., Bailey, S. C. C., and Smits, A. J.: Logarithmic scaling of turbulence in smooth- and rough-wall pipe flow, Journal of Fluid Mechanics, 728, 376–395, https://doi.org/10.1017/jfm.2013.255, 2013.

Iovieno, M., Cavazzoni, C., and Tordella, D.: A new technique for a parallel dealiased pseudospectral Navier–Stokes code, Computer Physics Communications, 141, 365–374, https://doi.org/10.1016/S0010-4655(01)00433-7, 2001.

Kármán, T. V.: Mechanical similitude and turbulence, Nachrichten von der Gesellschaft der Wissenschaften zu Gottingen - Fachgruppe I (Mathematik), 5, 1–19, 1931.

Katul, G. G., Porporato, A., and Nikora, V.: Existence of k-1 power-law scaling in the equilibrium regions of wall-bounded turbulence explained by Heisenberg's eddy viscosity, Physical Review E, 86, 066 311, https://doi.org/10.1103/PhysRevE.86.066311, 2012.

Kolmogorov, A.: Local structure of turbulence in an incompressible viscous fluid at very high Reynolds numbers, Physics-Uspekhi, 734, 1–4, 1968.

Kravchenko, A. and Moin, P.: On the Effect of Numerical Errors in Large Eddy Simulations of Turbulent Flows, Journal of Computational Physics, 131, 310–322, https://doi.org/10.1006/jcph.1996.5597, 1997.

Kravchenko, A. A., Moin, P., and Moser, R. D.: Zonal embedded grids for numerical simulations of wall-bounded turbulent flows, Journal of Computational Physics, 423, 412–423, https://doi.org/10.1006/jcph.1996.0184, 1996.

Kumar, V.: Investingating the Diurnal and Spatial variability of flows in the Atmospheric Boundary Layer: A Lagre Eddy Simulation Study, Ph.D. thesis, The Johns Hopkins University, Baltimore, Maryland, 2007.

Kumar, V., Kleissl, J., Meneveau, C., and Parlange, M. B.: Large-eddy simulation of a diurnal cycle of the atmospheric boundary layer: Atmospheric stability and scaling issues, Water Resources Research, 42, 1–18, https://doi.org/10.1029/2005WR004651, 2006.

Lesieur, M. and Metais, O.: New Trends in Large-Eddy Simulations of Turbulence, Annual Review of Fluid Mechanics, 28, 45–82, https://doi.org/10.1146/annurev.fl.28.010196.000401, 1996.

Li, N. and Laizet, S.: 2DECOMP & FFT-A Highly Scalable 2D Decomposition Library and FFT Interface, Cray User Group 2010 conference, pp. 1–13, 2010.

Lilly, D.: Representation of small scale turbulence in numerical simulation experiments, Proceedings of the IBM Scientific Computing Symposium on Environmental Sciences, pp. 195–210, https://doi.org/10.5065/D62R3PMM, 1967.

Lu, H. and Porté-Agel, F.: A modulated gradient model for scalar transport in large-eddy simulation of the atmospheric boundary layer, Physics of Fluids, 25, 0–17, https://doi.org/10.1063/1.4774342, 2013.

Lu, H. and Porté-Agel, F.: On the Development of a Dynamic Non-linear Closure for Large-Eddy Simulation of the Atmospheric Boundary Layer, Boundary-Layer Meteorology, 151, 1–23, https://doi.org/10.1007/s10546-013-9906-y, 2014.

Margairaz, F., Calaf, M., Giometto, M. G.: fmargairaz/LES-Utah: LES-Utah-momentum, Zenodo. https://doi.org/10.5281/zenodo.1048338, 2017.

Mason, P. J. and Thomson, D. J.:Stochastic backscatter in large-eddy simulations of boundary layers, Journal of Fluid Mechanics, 242, 51–78 https://doi.org/10.1017/S0022112092002271, 1992.

Mason, P. J.: Large-eddy simulation: A critical review of the technique, Quarterly Journal of the Royal Meteorological Society, 120, 1–26, https://doi.org/10.1002/qj.49712051503, 1994.

Meneveau, C., Lund, T. S., and Cabot, W. H.: A Lagrangian dynamic subgrid-scale model of turbulence, Journal of Fluid Mechanics, 319, 353–385, https://doi.org/10.1017/S0022112096007379, 1996.

Moeng, C. and Sullivan, P. P.: Large-Eddy Simulation, in: Encyclopedia of Atmospheric Sciences, pp. 232–240, Elsevier, https://doi.org/10.1016/B978-0-12-382225-3.00201-2, 2015.

Moeng, C.-H.: A large-eddy-simulation model for the study of planetary boundary-layer turbulence, Journal of the Atmospheric Sciences, 41, 2052–2062, https://doi.org/10.1175/1520-0469(1984)041<2052:ALESMF>2.0.CO;2, 1984.

Moeng, C.-H. and Wyngaard, J. C.: Spectral Analysis of Large-Eddy Simulations of the Convective Boundary Layer, Journal of the Atmospheric Sciences, 45, 3573–3587, https://doi.org/10.1175/1520-0469(1988)045<3573:SAOLES>2.0.CO;2, 1988.

Moin, P. and Kim, J.: Numerical investigation of turbulent channel flow, Journal of Fluid Mechanics, 118, 341–377, https://doi.org/10.1017/S0022112082001116, 1982.

Moore, G. E.: Cramming more components onto integrated circuits (Reprinted from Electronics, pg 114-117, April 19, 1965), Electronics, 38, 114–117, https://doi.org/10.1109/N-SSC.2006.4785860, 1965.

Moser, R. D. R., Moin, P., and Leonard, A.: A spectral numerical method for the Navier-Stokes equations with applications to Taylor-Couette flow, Journal of Computational Physics, 52, 524–544, https://doi.org/10.1016/0021-9991(83)90006-2, 1983.

Munters, W., Meneveau, C., and Meyers, J.: Shifted periodic boundary conditions for simulations of wall-bounded turbulent flows, Physics of Fluids, 28, 025 112, https://doi.org/10.1063/1.4941912, 2016.

Najm, H. N.: Uncertainty Quantification and Polynomial Chaos Techniques in Computational Fluid Dynamics, Annual Review of Fluid Mechanics, 41, 35–52, https://doi.org/10.1146/annurev.fluid.010908.165248, 2009.

Orszag, S. A.: Analytical theories of turbulence, Journal of Fluid Mechanics, 41, 363, https://doi.org/10.1017/S0022112070000642, 1970.

Orszag, S. A.: On the Elimination of Aliasing in Finite-Difference Schemes by Filtering High-Wavenumber Components, https://doi.org/10.1175/1520-0469(1971)028<1074:oteoai>2.0.co;2, 1971.

Orszag, S. A.: Comparison of Pseudospectral and Spectral Approximation, Studies in Applied Mathematics, 51, 253–259, https://doi.org/10.1002/sapm1972513253, 1972.

Orszag, S. A. and Pao, Y.-H.: Numerical Computation of Turbulent Shear Flows, in: Turbulent Diffusion in Environmental Pollution, Proceedings of a Symposium held at Charlottesville, edited by Frenkiel, F. N. and Munn, R. E., vol. 18, Part A of *Advances in Geophysics*, pp. 225–236, Elsevier, https://doi.org/10.1016/S0065-2687(08)60463-X, 1975.

Patterson, G. S.: Spectral Calculations of Isotropic Turbulence: Efficient Removal of Aliasing Interactions, Physics of Fluids, 14, 2538–2541, https://doi.org/10.1063/1.1693365, 1971.

Patton, E. G., Sullivan. P. P., Shaw, R. H., Finnigan, J. J., and Weil, J. C.: Atmospheric Stability Influences on Coupled Boundary Layer and Canopy Turbulence, Journal of the Atmospheric Sciences, 73, 1621–1647, https://doi.org/10.1175/JAS-D-15-0068.1, 2016

Piomelli, U.: Large-eddy simulation: achievements and challenges, Progress in Aerospace Sciences, 35, 335–362, https://doi.org/10.1016/S0376-0421(98)00014-1, 1999.

Porté-Agel, F., Meneveau, C., and Parlange, M. B.: A scale-dependent dynamic model for large-eddy simulation: application to a neutral atmospheric boundary layer, Journal of Fluid Mechanics, 415, 261–284, https://doi.org/10.1017/S0022112000008776, 2000.

Prandtl, L.: Zur Turbulenten Strömung in Rohren und langs Glätten, Ergebnisse der Aerodynamischen Versuchsanstalt zu Göttingen, B. 4, 18–29, 1932.

Raupach, M. R., Antonia, R. A., and Rajagopalan, S.: Rough-Wall Turbulent Boundary Layers, Applied Mechanics Reviews, 44, 1, https://doi.org/10.1115/1.3119492, 1991.

Sagaut, P.: Large Eddy Simuation of Incompressible Flow, Springer, third edn., 2006.

Saiki, E. M., Moeng, C.-h., and Sullivan, P. P.: Large-Eddy Simulation of the stably stratified Planetary Boundary Layer, Boundary-Layer Meteorology, 95, 1–30, https://doi.org/10.1023/A:1002428223156, 2000.

Salesky, S. T., Chamecki, M., and Bou-Zeid, E.: On the Nature of the Transition Between Roll and Cellular Organization in the Convective Boundary Layer, Boundary-Layer Meteorology, pp. 1–28, https://doi.org/10.1007/s10546-016-0220-3, 2016.

Schlatter, P. and Örlü, R.: Turbulent boundary layers at moderate Reynolds numbers: inflow length and tripping effects, Journal of Fluid Mechanics, 710, 5–34, https://doi.org/10.1017/jfm.2012.324, 2012.

Shah, S. and Bou-Zeid, E.: Very-Large-Scale Motions in the Atmospheric Boundary Layer Educed by Snapshot Proper Orthogonal Decomposition, Boundary-Layer Meteorology, 153, 355–387, https://doi.org/10.1007/s10546-014-9950-2, 2014.

Skamarock, W., Klemp, J., Dudhi, J., Gill, D., Barker, D., Duda, M., Huang, X.-Y., Wang, W., and Powers, J.: A Description of the Advanced Research WRF Version 3, Technical Report, p. 113, https://doi.org/10.5065/D6DZ069T, 2008.

Smagorinsky, J.: General circulation experiments with primirive equations, Monthly Weather Review, 91, 99–164, https://doi.org/10.1175/1520-0493(1963)091<0099:GCEWTP>2.3.CO;2, 1963.

Stoll, R. and Porté-Agel, F.: Large-eddy simulation of the stable atmospheric boundary layer using dynamic models with different averaging schemes, Boundary-layer meteorology, 126, 1–28, https://doi.org/10.1007/s10546-007-9207-4, 2008.

Stull, R. B.: An Introduction to Boundary Layer Meteorology, Springer Netherlands, Dordrecht, https://doi.org/10.1007/978-94-009-3027-8, 1988.

Sullivan, P. P. and Patton, E. G.: The Effect of Mesh Resolution on Convective Boundary Layer Statistics and Structures Generated by Large-Eddy Simulation, Journal of the Atmospheric Sciences, 68, 2395–2415, https://doi.org/10.1175/JAS-D-10-05010.1, 2011.

Sullivan, P. P., McWilliams, J. C., and Moeng, C.-H.: A subgrid-scale model for large-eddy simulation of planetary boundary-layer flows, Boundary-Layer Meteorology, 71, 247–276, https://doi.org/10.1007/BF00713741, 1994.

Takahashi, D.: Forty years of Moore's Law, The Seattle Times, 2005.

Takizawa, K. and Tezduyar, T. E.: Multiscale space-time fluid-structure interaction techniques, in: Computational Mechanics, vol. 48, pp. 247–267, Springer-Verlag, https://doi.org/10.1007/s00466-011-0571-z, 2011.

Tseng, Y.-H., Meneveau, C., and Parlange, M. B.: Modeling Flow around Bluff Bodies and Predicting Urban Dispersion Using Large Eddy Simulation, Environmental Science & Technology, 40, 2653–2662, https://doi.org/10.1021/es051708m, 2006.

Voller, V. and Porté-Agel, F.: Moore's Law and Numerical Modeling, Journal of Computational Physics, 179, 698–703, https://doi.org/10.1006/jcph.2002.7083, 2002.

Wörner, M.: Numerical modeling of multiphase flows in microfluidics and micro process engineering: a review of methods and applications, Microfluidics and Nanofluidics, 12, 841–886, https://doi.org/10.1007/s10404-012-0940-8, 2012.

Zang, T. a.: On the rotation and skew-symmetric forms for incompressible flow simulations, Applied Numerical Mathematics, 7, 27–40, https://doi.org/10.1016/0168-9274(91)90102-6, 1991.